

# Modeling of IGFC system

CO<sub>2</sub> removal from the gas streams,  
using membrane reactors

Raido Huberg



UNIVERSITY OF ICELAND



University  
of Akureyri

# MODELING OF IGFC SYSTEM

CO<sub>2</sub> removal from the gas streams, using membrane reactors

Raido Huberg

A 30 credit units Master's thesis

Supervisors:

Dr. Robert Braun (Project advisor)

Dr. David Dvorak (Academic advisor)

Prof. Thorsteinn I. Sigfusson (Academic advisor)

A Master's thesis done at  
RES | the School for Renewable Energy Science  
in affiliation with  
University of Iceland &  
the University of Akureyri

Akureyri, February 2009

Modeling of IGFC System

CO<sub>2</sub> removal from gas streams, using membrane reactors

A 30 credit units Master's thesis

© Raido Huberg, 2009

RES | the School for Renewable Energy Science

Solborg at Nordurslod

IS600 Akureyri, Iceland

telephone: + 354 464 0100

[www.res.is](http://www.res.is)

Printed in 14/05/2009

at Stell Printing in Akureyri, Iceland

## ABSTRACT

In the following work, the different capture concepts of carbon dioxide from an IGFC power plant have been considered and analyzed. The main objective was to compare the net power output according to the different tail-gas processing concepts (oxy-combustion,  $H_2$ - and  $O_2$ -conducting membranes) and to compare the difference of output when  $CO_2$  is vented.

The first concept considered is an IGFC plant (integrated gasification gas combined cycle plant with a fuel cell) with oxy-combustion for oxidizing the remaining fuel in the anode tail-gas. The second and third concepts are  $H_2$ -conducting membranes, one with  $N_2$  and the other with air as sweep gas. The fourth concept involves an  $O_2$ -conducting membrane in which  $O_2$  permeates from the cathode side to the anode side without mixing the two streams with each other. Also a fifth concept was developed, where the anode and cathode flows are mixed and no  $CO_2$  capture takes place. In the presented dissertation, a model with zero- and one-dimensional (membrane model) computational parts was created to simulate and evaluate the capability of the IGFC plant using different means to capture carbon dioxide.

The efficiency and net power of the different tail-gas concepts were compared, assuming an IGFC plant with oxy-combustion for carbon dioxide capture as the baseline. The capture of carbon dioxide proved to have an efficiency and probably an investment cost penalty. A Carbon Tax (adopted in some countries like Sweden) proportional to the number of kilograms of carbon dioxide released in the environment is necessary to make the carbon dioxide capture economically feasible.

## PREFACE

This thesis report is a part of the Department of Energy National Energy Technology laboratory and Colorado School of Mines project for “Modeling, Analysis and Optimization of IGFC Systems”. The cooperation between The Colorado School of Mines and The School for Renewable Science in Iceland allowed me, Raido Huberg, to participate in this project and work on establishing the Solid Oxide Fuel Cell and the gas turbine (SOFC-GT) part of the IGFC system.

The purpose of this thesis report was to quantitatively evaluate the SOFC-GT portion of the IGFC system with different post-SOFC CO<sub>2</sub> removal concepts. These were oxy-combustion of the anode stream, H<sub>2</sub>-conducting membrane, O<sub>2</sub>-conducting membrane and also the mixing of the anode and cathode stream, in which CO<sub>2</sub> was vented. The goal of this thesis is to evaluate what effect these different concepts have on the net-power production of the overall system.

The project was done in The Colorado School of Mines in Golden, Colorado, USA; under the supervision of Dr. Robert Braun, who was the project advisor. In addition there were two academic advisors: Dr. David Dvorak, from the University of Maine, USA; and Dr. Thorsteinn I. Sigfusson from the University of Iceland in Iceland.

In addition to the previous people mentioned the following people are acknowledged who contributed to the thesis project:

- Dr. Neal Sullivan, Colorado School of Mines
- RES academic administration and faculty
- Sigrún Lóa Kristjánsdóttir, RES
- Students of RES
- Students of RES
- My family and friends

# TABLE OF CONTENTS

1	Introduction.....	1
1.1	Background Information .....	1
1.2	Recent Trends in Electrical Power Industry.....	3
1.2.1	CO <sub>2</sub> taxation.....	3
1.3	Overview of IGCC Technology .....	4
1.3.1	Large Commercial-Scale IGCC plants .....	5
1.4	Overview of SOFC technology .....	7
1.4.1	Fuel Cell Systems .....	9
1.4.2	Thermal regulation of the fuel cell.....	10
1.5	Bottoming Cycles.....	10
1.5.1	Regenerative Brayton Cycle .....	10
1.5.2	Rankine Cycle.....	12
1.5.3	Combined Brayton-Rankine Cycle .....	13
1.5.4	Comparison of the different bottoming cycles.....	15
1.6	CO <sub>2</sub> capture concepts .....	17
1.7	Membrane technologies .....	21
1.8	Aspen Plus [1.22] .....	21
1.9	Objectives.....	23
1.10	Methodology.....	23
1.11	Chapter References.....	24
2	Modeling of various co <sub>2</sub> capture strategies in the SOFC-gas turbine subsystem.....	26
2.1	SOFC modeling.....	28
2.2	SOFC model verification .....	31
2.3	Modeling of air compression.....	33
2.4	Modeling of CO <sub>2</sub> preparation for sequestration .....	34
2.5	Gas turbine modeling .....	36
2.6	Steam cycle (Rankine cycle) modeling .....	36
2.7	Modeling of H <sub>2</sub> -conducting membrane.....	38
2.8	Modeling of O <sub>2</sub> -conducting membrane.....	40
2.9	Parasitic losses from ASU.....	40
2.10	Modeling of oxy-combustion .....	41
2.11	Modeling of H <sub>2</sub> -conducting membrane reactor with N <sub>2</sub> as sweep gas.....	42

2.12	Modeling of H <sub>2</sub> -conducting membrane reactor with air as sweep gas .....	43
2.13	Modeling of O <sub>2</sub> -conducting membrane reactor .....	45
2.14	Net power output calculations .....	46
2.15	Inputs to the model .....	46
2.16	Chapter References .....	47
3	Results .....	48
Appendix A .....		1
	Methods to increase power .....	3
	Methods to improve efficiency .....	4
	Reverse Brayton cycle .....	4
	Description .....	5
	Processes of the Rankine cycle .....	6
	Real Rankine cycle (non-ideal) .....	6
	Regenerative Rankine cycle .....	7
	Appendix References .....	8

## LIST OF FIGURES

<i>Figure 1: Schematic of IGCC power plant [1.8]</i> .....	5
<i>Figure 2: A integrated IGCC configuration [1.11]</i> .....	7
<i>Figure 3: Schematic of H<sub>2</sub>-O<sub>2</sub> SOFC [1.13]</i> .....	8
<i>Figure 4: Regenerative Brayton Cycle Fuel Cell Power System [1.12]</i> .....	11
<i>Figure 5: Fuel Cell Rankine Cycle Arrangement</i> .....	12
<i>Figure 6: Rankine Cycle Thermodynamics</i> .....	13
<i>Figure 7: Combined Brayton-Rankine Cycle Fuel Cell Power Generation System</i> .....	14
<i>Figure 8: Combined Brayton-Rankine Cycle Thermodynamics</i> .....	14
<i>Figure 9: SOFC-GT with pre-fuel cell CO<sub>2</sub> capture [1.20]</i> .....	18
<i>Figure 10: SOFC-GT with post-fuel cell hydrogen oxidation [1.20]</i> .....	19
<i>Figure 11: SOFC-GT with OCM-afterburner [1.20]</i> .....	19
<i>Figure 12: Working principle of the WGSMT-afterburner [1.20]</i> .....	20
<i>Figure 13: Hybrid cycle with WGSMT-afterburner [1.20]</i> .....	20
<i>Figure 14: Hydrogen transport through Pd membranes [1.21]</i> .....	21
<i>Figure 15: Baseline IGFC System Configuration [2.1]</i> .....	27
<i>Figure 16: Fuel Cell model in Aspen Plus</i> .....	28
<i>Figure 17: Reactions in the Stoichiometric reactor (Aspen Plus)</i> .....	29
<i>Figure 18: Specifications of the Stoichiometric reactor (Aspen Plus)</i> .....	29
<i>Figure 19: Fuel Cell model in Aspen Plus</i> .....	32
<i>Figure 20: Air compression for the fuel cell and for the ASU (Aspen Plus)</i> .....	34
<i>Figure 21: Specifications of the compressor model (Aspen Plus)</i> .....	34
<i>Figure 22: Preparation of CO<sub>2</sub> for storage (Aspen Plus)</i> .....	35
<i>Figure 23: Gas turbine model (Aspen Plus)</i> .....	36
<i>Figure 24: Gas turbine model specifications (Aspen Plus)</i> .....	36
<i>Figure 25: HRSG model (Aspen Plus)</i> .....	37
<i>Figure 26: H<sub>2</sub> conducting membrane</i> .....	39
<i>Figure 27: O<sub>2</sub> conducting membrane (Aspen Plus)</i> .....	40
<i>Figure 28: Oxy-combustor</i> .....	41
<i>Figure 29: Concept of H<sub>2</sub>-conducting membrane reactor with N<sub>2</sub> as sweep gas</i> .....	42
<i>Figure 30: Concept of H<sub>2</sub>-conducting membrane reactor with air as sweep gas</i> .....	43
<i>Figure 31: Concept of O<sub>2</sub>-conducting membrane reactor</i> .....	45
<i>Figure 32: Flow sheet of IGFC (CO<sub>2</sub> capture)</i> .....	48
<i>Figure 33: Flow sheet of IGFC (venting of CO<sub>2</sub>)</i> .....	49



<i>Figure 34: H<sub>2</sub> recovery [%]</i> .....	50
<i>Figure 35: CO<sub>2</sub> fraction in the exhaust</i> .....	52
<i>Figure 36: Net power production</i> .....	52
<i>Figure 37: Power production breakdown</i> .....	53
<i>Figure 38: Power consumption breakdown</i> .....	53
<i>Figure 39: Efficiency breakdown</i> .....	54
<i>Figure 40: Idealized Brayton Cycle [1.15]</i> .....	2
<i>Figure 41: Brayton Cycle (Gas Turbine) Efficiency</i> .....	2
<i>Figure 42: Brayton Cycle (Gas Turbine) Specific Power Output</i> .....	3
<i>Figure 43: Engine with a Rankine cycle [1.18]</i> .....	5
<i>Figure 44: T-s diagram of a typical Rankine cycle operating between pressures of 0,06 bar and 50 bar</i> .....	6
<i>Figure 45: Rankine cycle with superheat</i> .....	7
<i>Figure 46: Regenerative Rankine cycle</i> .....	8

## LIST OF TABLES

<i>Table 1: Estimated emissions of CO<sub>2</sub> from power generation using fossil fuels [1.6].....</i>	<i>2</i>
<i>Table 2: Stream properties of syngas after cleaning processes from a Destec entrained bed gasifier [1.12] .....</i>	<i>4</i>
<i>Table 3: Comparison of efficiencies [1.12] .....</i>	<i>5</i>
<i>Table 4: Table of Commercial-Scale coal/petroleum coke based IGCC power plants [1.5]....</i>	<i>6</i>
<i>Table 5: Performance Computations for Various High Temperature Fuel Cell (SOFC) Heat Recovery Arrangements [1.12].....</i>	<i>15</i>
<i>Table 6: Input and comparison of anode outputs of the two SOFC models.....</i>	<i>33</i>
<i>Table 7: Flows of the cathode.....</i>	<i>33</i>
<i>Table 8: Heat duties and <math>P_{DC}</math>.....</i>	<i>33</i>
<i>Table 9: Content and other parameters of syngas and air fed to the system.....</i>	<i>46</i>
<i>Table 10: Split fraction of cathode air recycled .....</i>	<i>50</i>
<i>Table 11: Properties of to the gas turbine .....</i>	<i>51</i>
<i>Table 12: CO<sub>2</sub> for sequestration.....</i>	<i>51</i>
<i>Table 13: Overall efficiency [%] .....</i>	<i>54</i>

# 1 INTRODUCTION

Fuel Cell technologies are maturing and currently in a pre-commercial stage. The main advantage of fuel cells is their ability to perform energy conversions with high efficiencies; extending the limited amount of resources and decreasing energy-related emissions. In addition to the higher efficiency fuel cells are scalable, making them suitable for a wide variety of applications, from powering a mobile phone to power plants.

Fuel Cells have been studied extensively, but mainly from the electrochemical and materials viewpoint. There is a lack of system level research especially for Integrated Gasification Fuel Cell (IGFC) System applications with CO<sub>2</sub> capture. When applying Fuel Cells in coal fired power plants with the Integrated Gasification Combined Cycles (IGCC), high-energy conversion efficiencies can be achieved. This can lead to higher maximum system efficiency and cost effectiveness. In order to reach these goals, methodologies for system-level optimal design must be developed.

The goal of this thesis report is to model and evaluate an Integrated Gasification Fuel Cell (IGFC) combined cycle power system, which uses syngas from a coal gasification plant, which captures and removes CO<sub>2</sub> for sequestration. The focus of this work is on quantitative evaluation of various CO<sub>2</sub> capture strategies in the SOFC-gas turbine subsystem.

Chapter one gives a background overview for the IGFC, to explain the project. A summary of the problem is presented (climate change caused by the CO<sub>2</sub> emissions and one of the tools to tackle that- the carbon tax- is explained). A short overview of integrated gasification combined cycle (IGCC) and SOFC technology is given, and the concepts of different CO<sub>2</sub> capture technologies are discussed. Various bottoming cycles are presented, and in addition, background information about other important parts of the systems is given.

In chapter two the main focus is the description of the model. Emphasis is given to how the model was created for the thesis, what assumptions were made, and in addition it is described how the SOFC model was verified.

In chapter three the results of the model are presented. In addition the results are discussed and possible improvements are suggested.

## 1.1 Background Information

Global climate change concerns associated with increasing anthropogenic CO<sub>2</sub> concentration in the atmosphere is providing the impetus for limiting green house gas emissions from power generation sources. One way to accomplish a reduction in greenhouse gases is through the introduction of a carbon tax. This will make coal fired power plants, the source of a significant amount of CO<sub>2</sub> and electric power, less competitive.

About 80% of the energy used world-wide comes from fossil fuels, and this is expected to increase until at least year 2020. The combustion of fossil fuels leads to emissions of CO<sub>2</sub> into the atmosphere, which is believed to contribute to undesired global warming.

The capture of CO<sub>2</sub> is easier from large stationary fossil fuel based power generation than in automotive applications, where emissions come from an enormous quantity of small, mobile

units. The current estimated, annual emissions of CO<sub>2</sub> world-wide from power plants using fossil fuels are shown in Table 1 [1.6]

Plant Type	Mt CO <sub>2</sub> /year (2000)
Coal	6276
Oil	992
Gas	1689
Total	8958

*Table 1: Estimated emissions of CO<sub>2</sub> from power generation using fossil fuels [1.6]*

The total recoverable reserves of coal around the world are estimated at 930 billion tons - reflecting in 2006 a reserves-to-production ratio of 143 [1.1]. Compared to other fossil fuels like oil and gas the reserves of coal are much more abundant and the prices are far less volatile compared to the prices of oil and gas.

41 percent of electricity is being produced in coal fired power plants and this number is predicted to increase slightly [1.2]. This growth is largely due to the rapid development of China where 70% of electricity is produced in coal fired power plants [1.7]. Coal power plants are the least carbon efficient power stations in terms of the level of carbon dioxide produced per unit of electricity generated [1.4].

Coal is, and will be in the future, a key ingredient in the total energy mix but it is also a major source of carbon dioxide, and in order to use these reserves without causing irreversible climate change the carbon has to be captured.

There are two main ways to decrease the carbon dioxide emissions per MW of power produced:

1. Increasing the overall efficiency of the plant
2. Capturing the CO<sub>2</sub> from the exhaust

In this particular study both are applied. The efficiency of the plant will be increased by applying gasifiers, a combined Brayton-Rankine cycle and an SOFC. The CO<sub>2</sub> from the exhaust can be captured in many ways; here oxy-combustion and different membranes are used (H<sub>2</sub>- and O<sub>2</sub>-conducting membranes).

Solid oxide fuel cells would be more suitable for integration to power cycles, because of their higher operating temperature, than some other fuel cells, proton exchange membranes (PEM) for example. One question in the design of IGFC power plants is how to couple coal gasification with the SOFC-gas turbine system. The SOFC (800-1000°C) and the gasifier (1200°C) operate at different temperatures and before the syngas from the gasifier enters the SOFC it goes through several cleaning processes during which the temperature is altered.

Thermal gradients within the ceramic SOFC stack must be relatively small (~150°C) to minimize thermally-induced stress. In addition the cell may be poisoned by some of the components (e.g., H<sub>2</sub>S) in the syngas, resulting in a fast and irreversible degradation in performance.

Currently, CO<sub>2</sub> removal is performed with a CO<sub>2</sub>-selective solvent at around 50°C. This makes thermal integration more complex and diminishes the efficiency. Also, steam is

needed for desorption processes. This results in a high price per ton of CO<sub>2</sub> removed. The emerging high temperature technology of membrane reactors is expected to offer a higher efficiency during gas separation.

## **1.2 Recent Trends in Electrical Power Industry**

It has been realized that human caused CO<sub>2</sub> emissions may increase the earth's average surface temperature, which affects the climate. In order to prevent this from happening, CO<sub>2</sub> emissions have to be decrease significantly. One possible tool to accomplish that is the introduction of a carbon tax. This should make the more polluting technologies more expensive and make the less polluting technologies, which are more expensive, more attractive. In addition this would motivate the coal fired power plants, for example, to do something to reduce their CO<sub>2</sub> emissions. If it is cheaper to capture the CO<sub>2</sub> than to pay the CO<sub>2</sub> tax, the plants will work to implement coal capture technologies.

Recent trends in the world show that new coal fired power plants are built rapidly, especially in China and India, where the economy is growing very fast. The reason for choosing coal is that it is a cheap and abundant energy source. And developing countries will use coal, and are already using it, extensively to meet the increasing demand for power.

### **1.2.1 CO<sub>2</sub> taxation**

A carbon tax is a tax on the carbon content of fuels — effectively a tax on the carbon dioxide emissions from burning fossil fuels.

Carbon atoms are present in every fossil fuel — coal, oil and gas. When a fossil fuel is burned the majority of the carbon is converted into CO<sub>2</sub>. Currently all carbon dioxide that is produced is vented to the atmosphere and remains there for some 20 years, trapping heat re-radiated from the Earth's surface and causing the so-called greenhouse effect, which is believed to be the main contributor to climate change.

A carbon tax (or CO<sub>2</sub> tax) would motivate power plants and companies to decrease their carbon dioxide emissions. There are several ways to decrease the carbon dioxide emissions per MW of power produced:

1. More efficient energy conversion
2. Carbon capture and sequestration
3. The use of non-carbon based energy resources (wind, solar, geothermal etc)

The emissions from coal fired power plants are the “dirtiest”. This means that compared to other fossil fuel technologies (gas turbine), significantly more CO<sub>2</sub> is being emitted per MW of power produced. At present there is very little taxation of carbon, thus the prices, for example of electricity and gasoline, do not include the costs of climate change. A carbon tax is considered an essential tool for taking action against climate change.

The reason for a carbon tax is simple: the levels of CO<sub>2</sub> in the Earth's atmosphere are destabilizing established climate patterns and threatening ecosystems. Large and rapid reductions in the world's carbon emissions are essential to preventing irreversible climate change and the resulting severe weather events, flooding of coastal areas etc.

So far carbon taxes have not been implemented widely. The first country to have a carbon tax was Finland in 1991 [1.10]. Other countries have since followed suit. In the EU the carbon tax is in the transition phase in order to prepare the energy sector.

### 1.3 Overview of IGCC Technology

The gasification of coal has been around since the end of the 18<sup>th</sup> century [1.11]. It was used to produce town gas for lighting and cooking until being replaced by electricity and natural gas by the beginning of the 19<sup>th</sup> century.. The main advantages of gasification are the flexibility in feedstock (coal, biomass, coke etc) and the products (electricity, chemicals, steam etc). Gasification of abundant coal can be an alternative to commercial coal based combustion systems and can be more efficient and environmental friendly.

The first commercial IGCC plants in the U.S. were put into service through the DOE's cooperative Clean Coal Technology (CCT) program, and have proven to be capable of exceeding even the most stringent emissions regulations currently applicable to coal-fueled power plants. Very low levels of pollutant air emissions (NO<sub>x</sub>, SO<sub>x</sub>, CO, PM10) have been achieved comparing to any other coal fueled power plant in the world. But IGCC plants are considered to be a first-of-its-kind technology and it will take time for IGCC's to experience wide spread use.

The heart of any gasification-based system is the gasifier, which can process a wide variety of feedstocks into gaseous products (mostly CO and H<sub>2</sub>) at high temperature and (usually) elevated pressure in the presence of oxygen and steam. In a gasifier the feedstock is not completely burned but only partially oxidized, and as a result the product, the syngas, consists mainly of H<sub>2</sub> and CO (Table 2). The same syngas was used in the developed model, which is described later in this report.

Temp [°C]	Pressure [atm]	CH <sub>4</sub> [%]	CO [%]	CO <sub>2</sub> [%]	H <sub>2</sub> [%]	H <sub>2</sub> O [%]	H <sub>2</sub> S [%]
399	15	0,3	42,3	9,6	35,8	10,3	trace

*Table 2: Stream properties of syngas after cleaning processes from a Destec entrained bed gasifier [1.12]*

The content of the cleaned syngas is suitable to feed directly to an SOFC. At this point the temperature of the gas has to higher at the anode inlet, in this study it was chosen to be 650°C.

IGCC technology is one of the most efficient and cleanest of available technologies for fossil-based power generation. The core process, gasification, is a commercially proven technology that has been deployed on a worldwide basis for the refining, chemical, and power industries. There are at least 163 commercial gasification plants in operation, under construction, or in planning and design stages around the world. The future holds that more gasification plants are being planned for power production.

Although there are numerous gasifiers operating commercially worldwide, there is far less experience with commercial operation of IGCC plants. In 2002 there were eleven major IGCC plants operating internationally that use coal, petroleum coke, and refinery residue as feedstock.

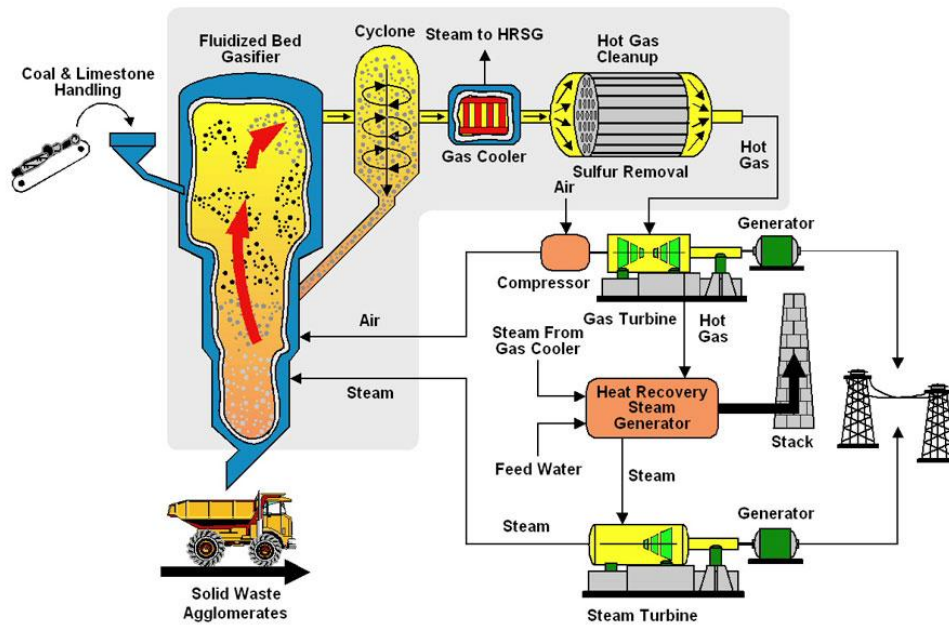


Figure 1: Schematic of IGCC power plant [1.8]

The main technology drivers for gasification are the feedstock and product flexibility, because all carbon-containing materials can be readily gasified and turned into clean syngas. In addition the high-pressure operation makes the products from the gasifier more amenable to cleaning. High-pressure also gives smaller volumes of flow with higher contents of species for processing. In contrast, the volume of flue gas from a combustion-based power plant is 40-60 times greater.

Advantages compared to other coal combustion technologies include:

1. Less CO<sub>2</sub> per unit of energy because of higher overall efficiency
2. Discharge of solid waste/by-products and wastewater is lower
3. Recovery of high-value-added by-products or co-products[1.12]

	IGCC Plant	PC Plant	FBC Plant
Thermal Efficiency, % (HHV Basis)	38-50	34-42	36-45

\*PC – pulverized coal, FBC – fluidized bed combustion

Table 3: Comparison of efficiencies [1.12]

As we can see from table 3 the efficiency of the IGCC is comparable with the conventional technologies. Nevertheless IGCC offers some additional advantages and makes IGCC the technology of choice.

### 1.3.1 Large Commercial-Scale IGCC plants

Experience in operating IGCC has been gained through several commercial-scale demonstration power plants in the United States and in Europe.

PLANT NAME	PLANT LOCATION	OUTPUT (MWe)	FEEDSTOCK	GASIFIER TYPE	POWER ISLAND	OPERATION STATUS
Texaco Cool Water	Daggett, CA, USA	125	Bituminous Coal (1000 tpd)	Texaco	CCGT-GE 7FE	1984-1988
Dow Chemical/Destec LGTI Project	Paquemine, LA, USA	160	Subbituminous Coal (2200 tpd)	E-Gas (formerly Destec)	CCGT-Westinghouse 501	1987-1995
Tampa Electric Polk Plant	Polk County, FL, USA	250	Bituminous Coal (2200 tpd)	Chevron Texaco	CCGT-GE 7FA	1996-Present
PSI Energy/Global Energy Wabash River Plant	West Terre Haute, IN, USA	262	Bituminous Coal and Petroleum Coke (2544 tpd)	E-Gas (formerly Destec)	CCGT-GE 7FA	1995-Present
NUON/Demkolec/Willem-Alexander	Buggenum, The Netherlands	253	Bituminous Coal	Shell	CCGT-Siemens V94.2	1994-Present
ELCOGAS/Puertollano	Puertollano, Spain	298	Coal and Petroleum Coke (2500 tpd)	Prenflo	CCGT-Siemens V94.3	1998-Present

CCGT-Combined Cycle Gas Turbine, tpd-short tons per day

*Table 4: Table of Commercial-Scale coal/petroleum coke based IGCC power plants [1.5]*

The first two U.S. plants listed in the table, Cool Water and LGTI (Louisiana Gasification Technology Inc Project), were important first-generation, large-scale IGCC projects that demonstrated the major IGCC characteristics of low emissions and stable integrated control of the gasification process with a combined cycle in a power utility setting. Both of these projects were funded with guaranteed product price support and were shut down once the duration of the price guarantee period expired.

The rest of the plants listed, are second-generation, which is the current generation. These IGCC systems have been improved according to what was learned from the initial plants. The plants in Europe make use of different gasifier designs and turbine vendors.

Each of the four major commercial-sized, coal/coke-based IGCC demonstration plants currently in operation use a different gasification technology, gas cooling and gas cleanup arrangement, and integration scheme between the plant units. All of the current coal based plants integrate the steam systems of the gasification and power block sections.

The major difference between the plants in Europe and in the US is the degree of integration between the gas turbine and the air separation unit (ASU). The different degree of integration is derived from the different objectives of the plants. In Europe the main goal is to increase the efficiency because of the higher prices of fuel, while in the US the main objective is the availability of the technology.

The European demonstration plants are both highly integrated designs with all the air for the ASU being taken as a bleed of extraction air from the combustion turbine compressor. In contrast, the operating U.S. plants are less integrated, and the ASUs have their own separate air compressors. A more tightly integrated ASU design, like that found in the European plants, results in higher plant efficiency. However, there is a potential loss of plant availability and operating controllability for the highly integrated system, and the higher degree of integration requires a longer start-up time. Fig 2 presents a block flow diagram that identifies the difference between the integration schemes.



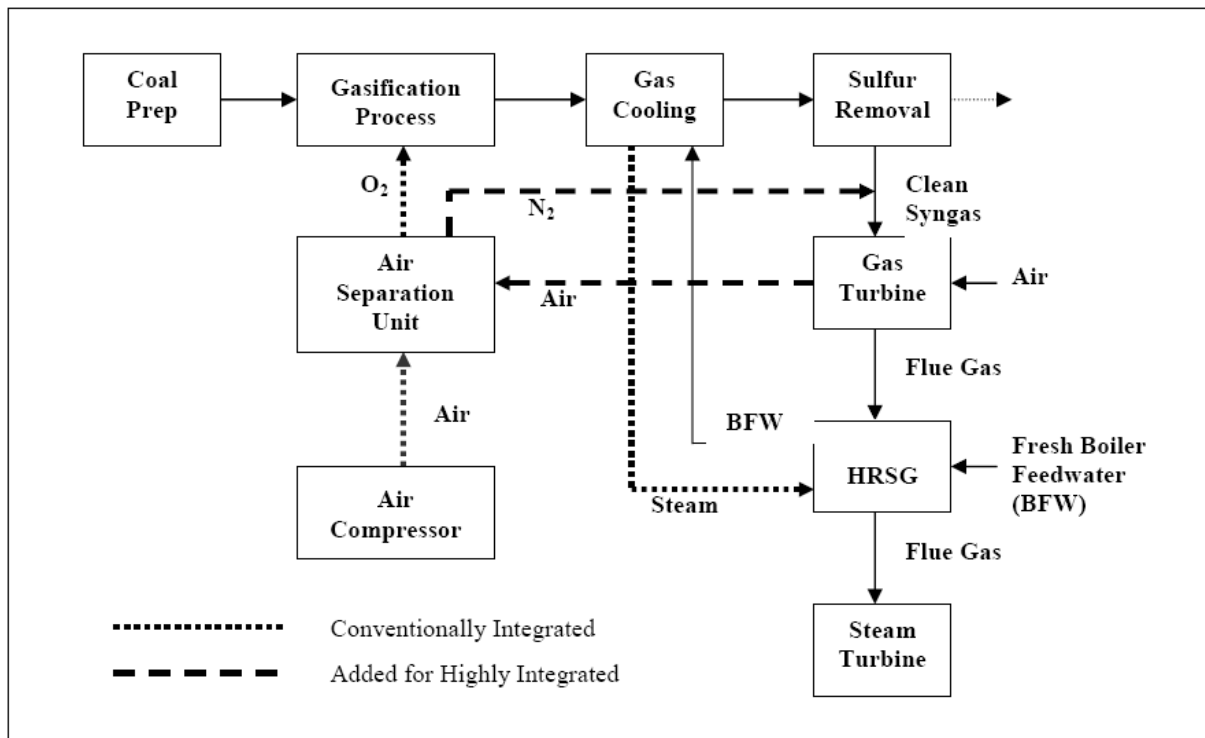
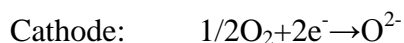
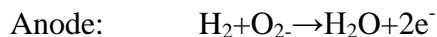


Figure 2: A integrated IGCC configuration [1.11]

In Europe efficiency is a major concern that has led to capital investment for the tightly integrated plant because of the high prices of fuel. In the U.S., fuel prices are lower and availability is a more important factor than efficiency. It is now the general consensus among IGCC plant designers that the preferred design is an intermediate approach; one in which the ASU derives part of its air supply from the gas turbine compressor and part from a separate dedicated compressor. This provides the necessary flexibility for quicker start up, less usage of expensive secondary fuels, and an auxiliary power load intermediate between the two options.

## 1.4 Overview of SOFC technology

Solid oxide fuel cells (SOFCs) have a solid electrolyte, non-porous metal oxide, most commonly it is made of yttria-stabilized zirconia (YSZ) which is an oxygen ion (oxygen vacancy) conductor. Here the  $O^{2-}$  is the mobile conductor and the anode and cathode reactions are as follows:



In the case of an SOFC, water is produced on the anode, rather than at the cathode side, as in a proton exchange membrane fuel cell (PEMFC).

The cell operates at 600-1000 °C. The reason for this high operating temperature is that at lower temperatures the solid electrolyte material does not conduct oxygen ions, or if it does it

happens at a low rate. The anode and cathode materials are different. Typically, the anode is a Ni-ZrO<sub>2</sub> cermet (must withstand highly reducing high-temperature environment) and the cathode (must withstand highly oxidizing high-temperature environment) is Sr-doped LaMnO<sub>3</sub>. There is no liquid electrolyte with its attendant material corrosion or electrolyte management problems. The cell is constructed with two porous electrodes that sandwich an electrolyte. Air flows along the cathode. When an oxygen molecule contacts the cathode/electrolyte interface, it acquires electrons from the cathode. The oxygen ions diffuse into the electrolyte material and migrate to the other side of the cell where they contact the anode. The oxygen ions encounter the fuel at the anode/electrolyte interface and react catalytically, giving off water, carbon dioxide, heat, and electrons. The electrons transport through the external circuit, providing electrical energy.

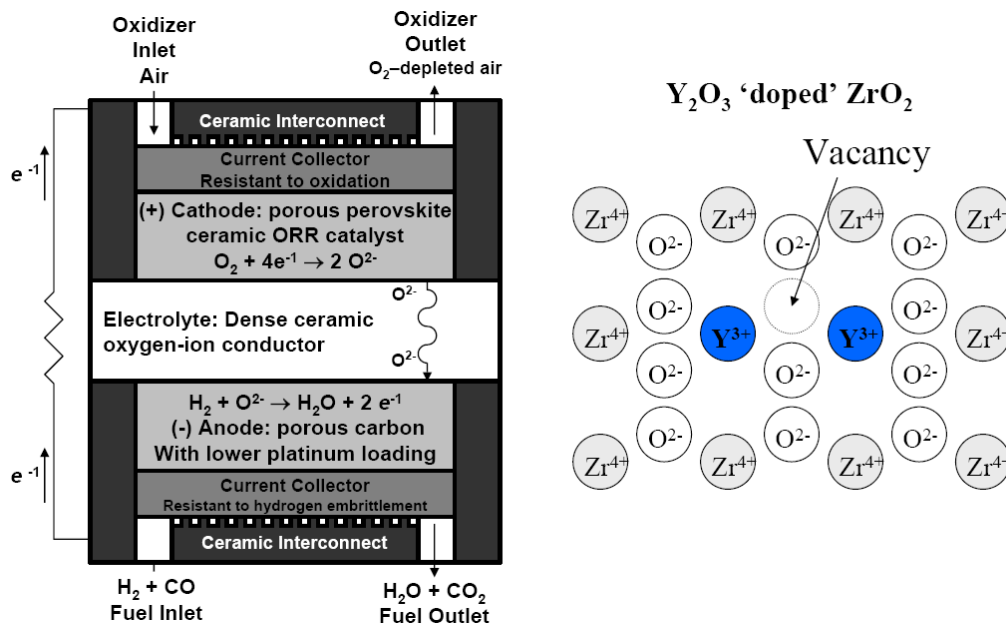


Figure 3: Schematic of H<sub>2</sub>-O<sub>2</sub> SOFC. A solid state ceramic is the electrolyte. A nickel-YSZ cermet anode and a mixed conducting ceramic cathode provide the required thermal, mechanical, and catalytic properties at high SOFC operating temperatures. Water is produced at the anode [1.13]

The high temperature of the SOFC, however, places stringent requirements on its materials. The development of suitable low cost materials and the low-cost fabrication of ceramic structures are presently the key technical challenges facing SOFCs [1.12]. On the other hand their high operating temperature makes them more suitable for integration with Brayton, Rankine or Brayton-Rankine cycles. Following are listed the challenges and advantages of the high-temperature operation:

Advantages [1.14]:

- Fuel flexibility (internal reforming could simplify the system)
- Non-precious metal catalyst
- High quality waste heat for cogeneration applications (overall system efficiency can reach 90%)
- Solid electrolyte
- Relatively high power density
- High efficiency (about 50-60%)

Challenges:

- Significant high-temperature materials issues
- Sealing issues
- Relatively expensive components/fabrication
- Very long start-up period
- Conventional materials are easily fouled by sulphur

One possible way to overcome some of these challenges is an intermediate-temperature (400-700°C) SOFC. This could help reduce the cost of the fuel cell by requiring less-expensive materials and fabrication methods.

Solid oxide fuel cells (SOFC) allow the conversion of a wide range of fuels, including various hydrocarbon fuels. The relatively high operating temperature allows for highly efficient conversion to power, internal reforming, and high quality by-product heat for cogeneration or for use in a bottoming cycle. Indeed, both simple-cycle and hybrid SOFC systems have demonstrated among the highest efficiencies of any power generation system, combined with minimal air pollutant emissions and low greenhouse gas emissions. These exhibitions have made SOFC an attractive technology for stationary power generation in the 2 kW to 100s MW capacity range.

#### **1.4.1 Fuel Cell Systems**

Fuel cells are not 100% efficient and there is heat produced which must be removed. The excess heat can be utilized by integrating the SOFC into an energy system; there the heat can be used in the following ways:

1. Production of steam
2. Production of hot water
3. Converted to electricity via a gas turbine or steam bottoming cycle

The production of steam and/or hot water is called cogeneration. Cogeneration is applied when the rejected heat has low temperatures. For example, the steam produced by low temperature fuel cells, PEMFC or phosphoric acid fuel cell (PAFC), which operate at 90-210°C [1.14], will not have a very high pressure and this is not very suitable for a steam bottoming cycle. SOFC on the other hand, which operate at temperatures from 400 to 1000°C, are capable of producing steam in excess of 540°C [1.12]. But if the amount of heat is relatively small it is not reasonable to use it in a bottoming cycle, but it is reasonable to produce hot water for example.

Another option is to use some bottoming cycle for utilizing the excess heat. The bottoming cycle options are explained in chapter 1.5. Using a bottoming cycle makes sense when there is a significant amount of rejected heat available at high-temperatures. Adding a bottoming cycle can significantly increase the efficiency of electric generation. When the heat is accumulated in a high-pressure and temperature gas stream then a gas turbine potentially followed by a heat recovery steam generator and steam turbine should be considered. But if the hot gas stream is at low pressure, then a steam bottoming cycle would be more logical.

In system design and optimization one must consider many questions, issues, and trade-offs. For example having maximal electrical output may lead to lower overall efficiency and /or

higher operating and investment costs. The optimization depends on the objectives of the specific system. The objectives can include the following, individually or combined: power output, overall weight, fuel basis, emissions, cost etc. Site-and-application-specific criteria and conditions may strongly influence the cycle design criteria and resulting design.

#### **1.4.2 Thermal regulation of the fuel cell**

An significant amount of heat has to be removed from the fuel cell stack. Heat removal from fuel cells can be accomplished:

- Directly through the flow of reactants to and products from them.
- Indirectly through heat transfer surfaces in contact with the cell or included within a battery.

Some elements in the fuel cell system have a fixed range of operating temperature, thus it is necessary to remove heat in such a manner that temperatures are being kept within a certain range. If the heat is removed directly, by reactant flows, the temperatures are regulated by the quantity of flow of the reactants (usually air). In addition the cathode stream can be recycled to achieve the desired inlet temperatures of the air stream; this is done to avoid the use of excess energy for pre-heating the air. The recycling of the anode stream (fuel stream) is possible as well, but in the model for this thesis report the recycling of the cathode stream was used.

If heat is removed from the fuel cell indirectly, then the flow and temperature of the coolant stream can be selected somewhat independent of the cell operating temperature.

If air flow is chosen for cell cooling the air flow will be increased significantly, by a factor of 4-8 above that required for oxidation of the fuel. This will also lead to increased power consumed by the system because more air needs to be compressed. It is suggested to compare the power demand of direct and indirect cooling of the fuel cell stack. As it turns out, the optimization of the amount of air compressed for the system plays a big role on the overall power output.

### **1.5 Bottoming Cycles**

Basically there are three different kinds of bottoming cycles to choose from:

- Regenerative Brayton Cycle
- Combined Brayton-Rankine Cycle
- Rankine Cycle

In the next chapters these different bottoming cycles are described and compared with each other. All these bottoming cycles use methane ( $\text{CH}_4$ ) as fuel.

#### **1.5.1 Regenerative Brayton Cycle**

The regenerative Brayton cycle (Figure 4) shows a gas turbine compressor for the air (1) flow to the cell. The flow (2) is then passed through a countercurrent, recuperative heat exchanger to recover heat from the combustion product gases leaving the gas turbine (6). The air (3) and the fuel streams then pass into the cathode and anode compartments of the fuel cell(s). The air (4) and fuel streams leaving the cell(s) enter the combustor where they mix and the

residual fuel burns. The combustion products (5) enter the turbine, expand, and generate additional power. The turbine exhaust gases (6) pass through the recuperative exchanger to the stack. [1.12]

In addition the T-s diagram is presented in Figure 4. All the processes in different parts of the system are described through the T-s diagram.

The most significant variables characterizing the cycle are:

- the fuel cell operating temperature range
- temperature and pressure at the gas turbine expander inlet

These variables are related to other operating variables in the system. Like the fuel utilization, it is not optimal to react all the fuel in the fuel cell. The previous statement can be explained as follows; the fuel cell operating temperature range is around  $800^{\circ}\text{C}$  and by burning the unreacted fuel in a combustor the inlet temperature of the gas turbine can be raised.

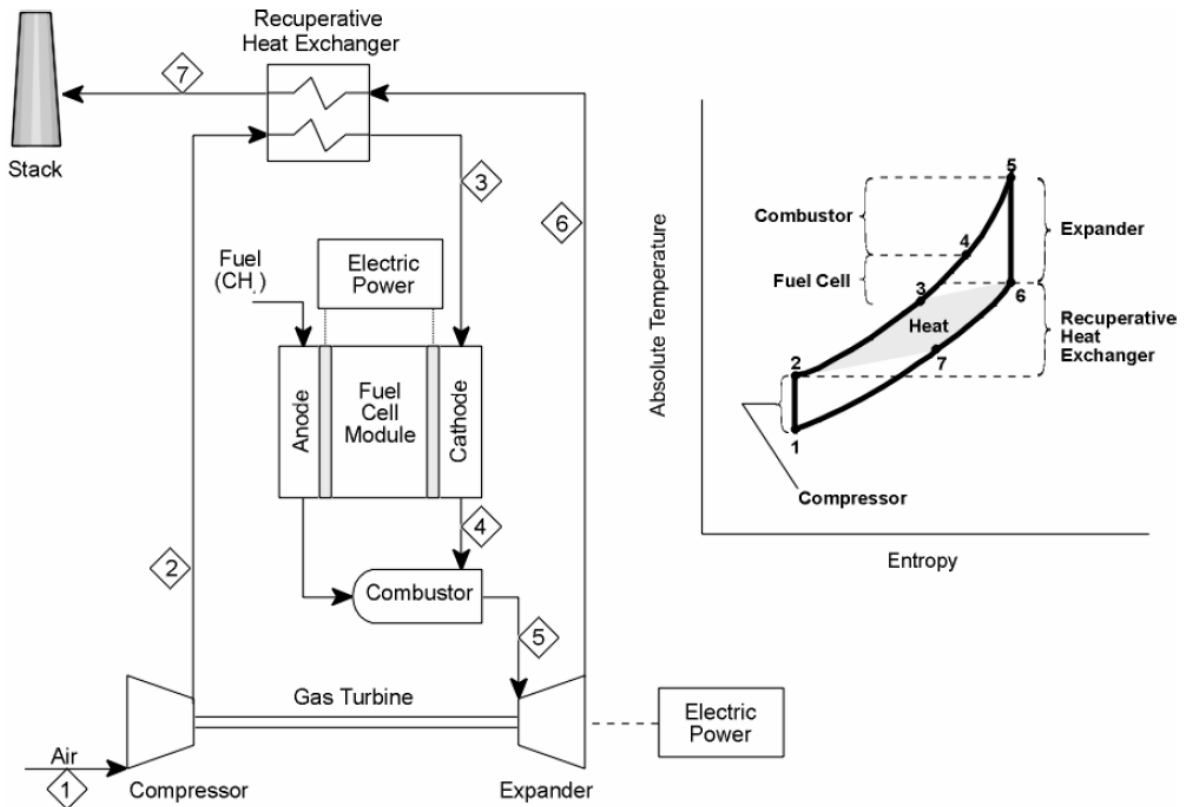


Figure 4: Regenerative Brayton Cycle Fuel Cell Power System [1.12]

Some of the following aspects have to be kept in mind by modeling this cycle:

- efficiency of the gas compressors
- efficiency of the turbine expander
- efficiency of the fuel cell
- pressure losses as the gases flow through the system
- the temperature differences
- the difference in heat capacities of the streams flowing through the recuperative heat exchanger



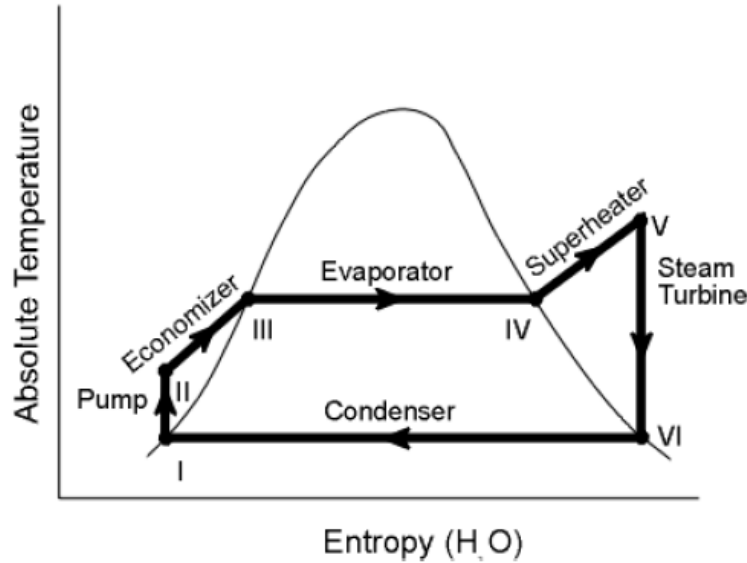


Figure 6: Rankine Cycle Thermodynamics

### 1.5.3 Combined Brayton-Rankine Cycle

The combined Brayton-Rankine cycle, Figure 7, again shows the gas turbine compressor for the air flow to the cell (2). This flow passes through a heat exchanger in direct contact with the cell; it removes the heat produced in cell operation and maintains cell operation at constant temperature. The air (3) and fuel streams then pass into the cathode and anode compartments of the fuel cell. The separate streams leaving the cell enter the combustor and then the gas turbine (5). The turbine exhaust (6) flows to the heat recovery steam generator and then to the stack (7). The steam produced (V) drives the steam turbine. It is then condensed (I) and pumped (II) back to the steam generator [1.12].

The desired fuel cell operating temperature is achieved by changing the air/fuel ratio entering the fuel cell; the same was done in the model created for this thesis report, where the air flow was adjusted according to the cooling necessity. The gas turbine nozzle inlet temperature (NIT) and pressure ratios (PR) are achieved by the selected fraction of the  $\text{CH}_4$  fuel consumed. These are selected to correspond with those of a conventional, large-scale, utility gas turbine.

The T-s diagrams of both the Brayton and the Rankine cycles are illustrated in Figure 8. The pressure and temperature increase during fuel and air compression (1-2) in this combined cycle will be significantly greater than in the regenerative Brayton cycle. The heating of the air and fuel (2-3), the operation of the fuel cell (3-4), and the burning of the residual fuel (4-5) are assumed to occur at constant pressure. The expansion of the combustion product gases in the gas turbine (5-6) is represented as an adiabatic, reversible (constant S) process. Next, heat is removed from these gases (6-7) at nearly constant pressure in the heat recovery steam generator; and they pass out through the stack (7-1).

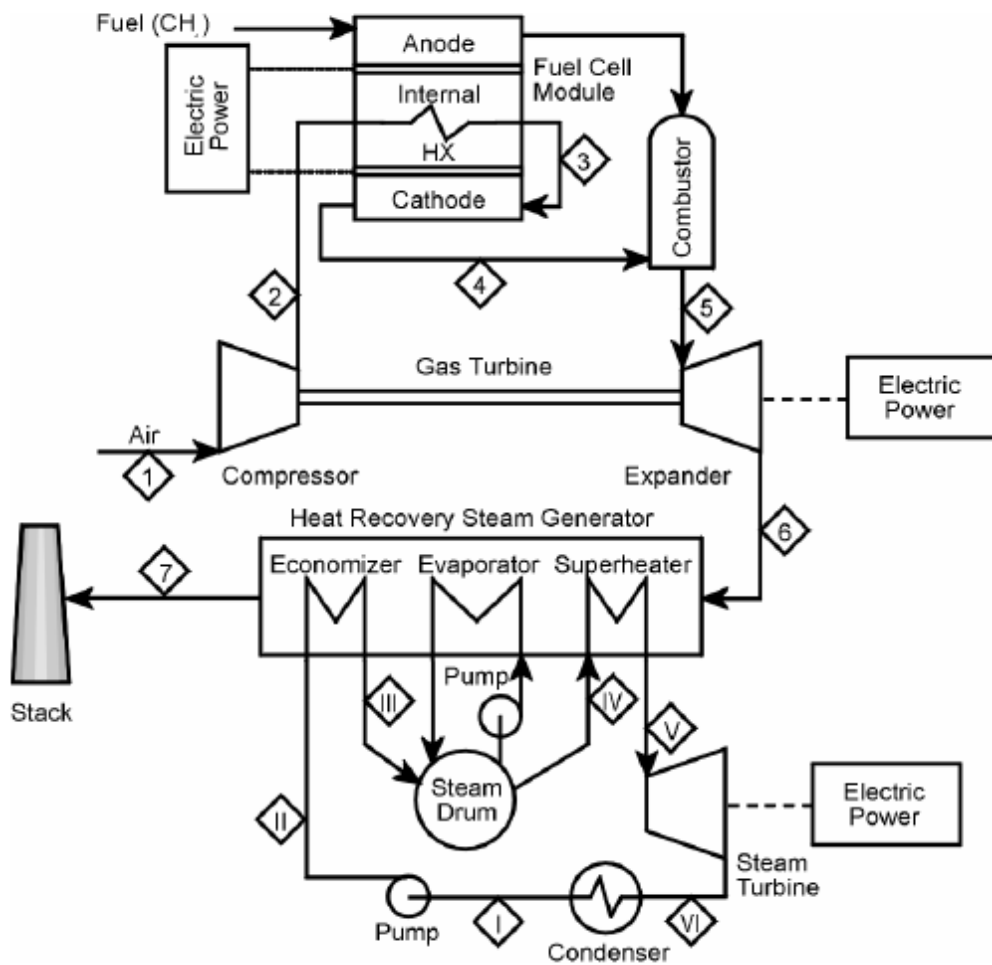


Figure 7: Combined Brayton-Rankine Cycle Fuel Cell Power Generation System

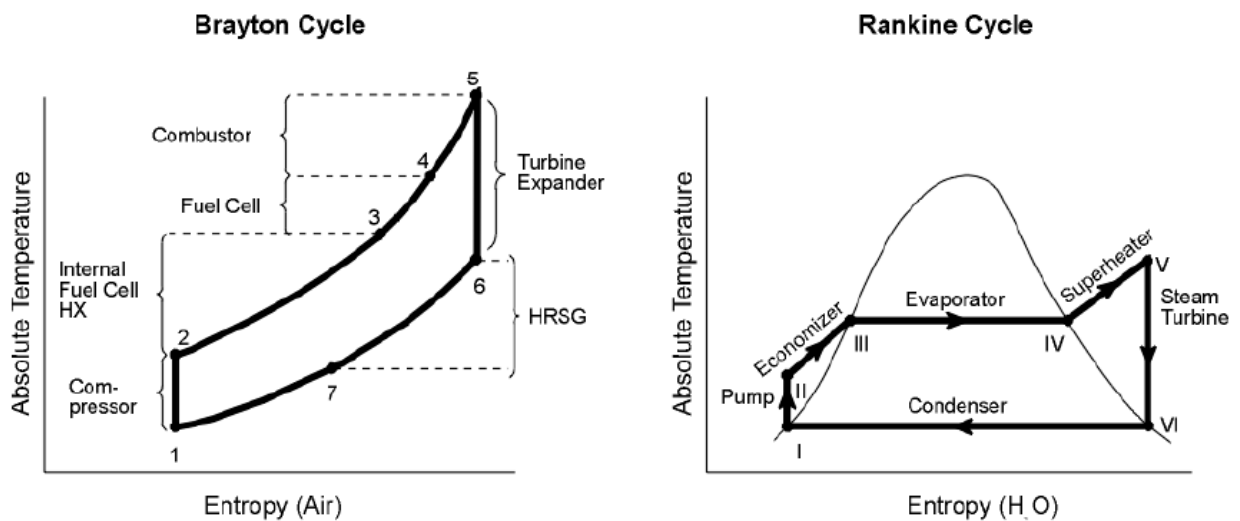


Figure 8: Combined Brayton-Rankine Cycle Thermodynamics

One thermodynamic advantage the Rankine bottoming cycle offers is the lowered temperature of heat rejection in the steam condenser, from the overall combined cycles.



The efficiency of the overall system is increased from 57 percent for the fuel cell alone to 75 percent for the overall system.

The link between the Brayton and the Rankine cycles is a heat recovery steam generator (HRSG). The heat of the used gas from the Brayton cycle has to be transferred to the water-steam inside the HRSG. The heat in the HRSG is utilized (Figure 8 Rankine cycle) in the economizer evaporator and superheater.

#### 1.5.4 Comparison of the different bottoming cycles

The regenerative Brayton cycle heat-fuel recovery arrangement is the simplest approach to heat recovery compared to the Brayton-Rankine combined cycle and the Rankine cycle.

The Rankine cycle heat-fuel recovery arrangement is less complex but also less efficient than the combined Brayton-Rankine cycle approach, and more complex and less efficient than the regenerative Brayton approach. On the positive side there is no need for a large, high temperature gas to gas heat exchanger and can provide a source of steam.

The combined Brayton-Rankine cycle heat-fuel recovery arrangement is significantly more complex and less efficient than the simple regenerative Brayton cycle approach. It does, however, eliminate the requirement for a large, high temperature gas to gas heat exchanger.

The effectiveness of the regenerative Brayton cycle performance will depend on the efficiency of the fuel cell, compressor, and turbine units; the pressure loss of gases flowing through the system; the approach temperatures reached in the recuperative exchanger; and, most importantly, the cost of the overall system.

The combined Brayton-Rankine cycle depends on both the fuel cell and the gas turbine components for conversion of the fuel and thus for its overall efficiency. The extent of conversion of the fuel occurring in the fuel cell increases as the cell operating temperature and the range of coolant temperature rise increase.

The fuel cell Rankine cycle arrangement has been selected so that all fuel preheating and reforming are carried out external to the cell and air preheating is accomplished by mixing with recycled depleted air. The air feed flow is adjusted so that no heat transfer is required in the cell or from the recycled air. Consequently, the internal fuel cell structure is greatly simplified, and the requirement for a heat exchanger in the recycled air stream is eliminated. [1.12]

In table 5 the efficiencies of the different heat recovery arrangements are presented, in addition to the efficiencies of the different power generating parts.

Heat Recovery Arrangement	Work Output, %			Overall System Eff., %
	Fuel Cell	Gas Turbine	Steam Turbine	
Regenerative Brayton Cycle	69,3	30,7	n/a	82,1
Regenerative Brayton Cycle	74,5	25,5		76,3
Combined Brayton-Rankine Cycle	75,3	10,3	14,3	75,6
Rankine Cycle	79,1		20,9	72,4

PR=pressure ratio of gas turbine, NIT=nozzle inlet temperature of the turbine expander

*Table 5: Performance Computations for Various High Temperature Fuel Cell (SOFC) Heat Recovery Arrangements [1.12]*

General Conditions:

- SOFC
- Operating temperature, 925-1050 °C
- Fuel cell output: 60% of theoretical maximum from CH<sub>4</sub> fuel
- Gas turbine compressor efficiencies: 83, 89%
- Steam turbine efficiency: 90%

All three approaches are more suitable for application to high temperature fuel cells, solid oxide fuel cell or molten carbonate fuel cell. Applying them for lower temperature fuel cells, PEMFC or PAFC, will severely limit the power generation and make it impractical.

All three of the heat recovery arrangements have calculated overall efficiencies greater than 70 percent as indicated in Table 5. None have been optimized in any sense - in terms of efficiency, capital and operating costs, maintainability or availability. All the arrangements have their advantages and disadvantages, which are described further in subsequent paragraphs.

It seems that the regenerative Brayton cycle is the simplest of them and has highest potential overall efficiency over the combined Brayton-Rankine and Rankine cycle approaches. However in this thesis report the combined Brayton-Rankine cycle was used; the reason for this was to get an idea of how much electric power could be produced.

Advantages and disadvantages of various fuel cell bottoming cycles [1.12]

### **Regenerative Brayton**

Advantages:

- Simple cycle arrangement, minimum number of components.
- Relatively low compressor and turbine pressure ratio, simple machines.
- Relatively low fuel cell operating pressure, avoiding the problems caused by anode/cathode pressure differential and high pressure housing and piping.
- Relatively low turbine inlet temperatures, perhaps 1065°C for solid oxide and 787°C for molten carbonate fuel cell systems. Turbine rotor blade cooling may not be required.
- Relatively simple heat removal arrangements in fuel cells, accomplished by excess air flow. No internal heat transfer surface required for heat removal.
- Fuel conversion in cells maximized, taking full advantage of fuel cell efficiency.
- Adaptability to small scale power generation systems.

Disadvantages:

- Tailoring of compressor and turbine equipment to fuel cell temperature and cycle operating pressure required. (It is not clear to what extent available engine supercharging and industrial compressor and turbine equipment can be adapted to this application.)
- Large gas to gas heat exchanger for high temperature heat recuperation required.
- Efficiency and work output of the cycle sensitive to cell, compressor, and turbine efficiencies; pressure losses; and temperature differentials.

## **Combined Brayton-Rankine**

Advantages:

- Integrated plant and equipment available for adaptation to fuel cell heat recovery.
- High efficiency system for heat recovery.

Disadvantages:

- Complex, multi component, large scale system for heat recovery.
- Adaptation of existing gas turbine required to provide for air take off and return of hot depleted air and partially burned fuel.
- High pressure operation of the bulky fuel cell system required.
- Precise balancing of anode and cathode pressures required to prevent rupture of fuel cell electrolyte.
- Indirect heat removal required from fuel cells with compressed air, initially at low temperature, to enable significant conversion of the fuel flow in the cells.

## **Rankine**

Advantages:

- Ambient pressure operation within the fuel cell.
- Heat recovery in a boiler, avoiding the high temperature gas to gas exchanger of a regenerative Brayton cycle.
- No gas turbine required, only fans for air and exhaust product gas flow.
- Steam available for cogeneration applications requiring heat.

Disadvantages:

- Inherently lower efficiency than regenerative Brayton and combined Brayton-Rankine cycles.
- Requirement for cooling and feed water.
- Greater complexity than regenerative Brayton cycle arrangement.

## **1.6 CO<sub>2</sub> capture concepts**

For CO<sub>2</sub> capture several technologies like gas turbines, membranes and solid oxide fuel cells can be used. Commercially available CO<sub>2</sub> capture technologies for power conversion are in general post-combustion technologies; i.e. the CO<sub>2</sub> is captured from the flue gases after the conversion of fuel into power. Post-combustion CO<sub>2</sub> capture, however, results in a significant drop in efficiency and an increase in plant investment and operating costs. Typically, CO<sub>2</sub> capture with an amine absorption/desorption unit in a gas fired combined cycle results in an efficiency drop of 9%-points (steam is needed for the desorption process), an investment increase of more than 50% and a rise in cost per CO<sub>2</sub> captured. For coal fired power plants the penalties are even bigger. If the CO<sub>2</sub> stream is diluted (mainly with N<sub>2</sub>) the removal of CO<sub>2</sub> is much more complex.

In order to make CO<sub>2</sub> capture feasible the efficiency and financial penalties have to be reduced significantly. To achieve this new concepts are required. These concepts will have to make use of one or probably a combination of the technologies (gas turbines, membranes and fuel cells) mentioned above. In this work all these technologies are put together and different tail-gas concepts are evaluated.

The gas turbine is a well established technology mostly used to utilize natural gas. It can also be implemented to gasification-based power plants and used to burn H<sub>2</sub>. However, a physical or chemical absorption step is still required to separate the CO<sub>2</sub> from the hydrogen (separator on Figure 9).

Membranes may offer the potential for high-efficiency gas separation. Ceramic and metallic membranes are in focus because of their high operating temperature and pressure.

Membranes can be used not only as separation devices but possibly also as chemical reactors and may also act as heat exchangers; in this case they are called membrane reactors (MR). Membrane activity supports chemical reactions. For example a water-gas shift reaction is promoted when one of the products, hydrogen, is withdrawn constantly.

A drawback in membrane applications is that a difference in the partial pressure is required for species to permeate through the membrane and thus 100% recovery of hydrogen, for example from syngas, is not possible. To integrate a membrane and reactor into one device, syngas from a coal gasifier can be converted to hydrogen using a water-gas shift membrane reactor (WGSMR) which is then used for fuelling a gas turbine. A more integrated approach is also possible: integrating reforming, shift and membrane separation in one module, which is then placed in a gas turbine cycle.

Fuel cells, of which the SOFC is the most relevant to this study, offer high-efficiency power production. A special property of the SOFC, which makes it attractive for CO<sub>2</sub> separation, is that the fuel conversion takes place without the dilution of CO<sub>2</sub> with nitrogen and a high CO<sub>2</sub> content stream is formed. In addition to the high efficiency of the SOFC (50-60%), an additional gain in efficiency can be achieved by combining the SOFC with a gas turbine to form a hybrid system. Numerous approaches to achieving this result are possible.

A pre-fuel cell CO<sub>2</sub> capture concept can be seen in figure 9. If we have syngas coming from a gasifier as fuel, the reforming step can be left out. If we want to separate the CO<sub>2</sub> and H<sub>2</sub> before the SOFC, the entire CO in the syngas has to be shifted in the water-gas shift reaction. In this case a stream of H<sub>2</sub> and H<sub>2</sub>O enters the anode of the SOFC. The use of an amine based CO<sub>2</sub> removal is necessary. After separation the CO<sub>2</sub> can be compressed and stored. In addition, instead of the shift reactor and the separator a water-gas shift H<sub>2</sub>-selective membrane reactor can be used. A pre-fuel cell CO<sub>2</sub> capture concept will not be investigated in this work.

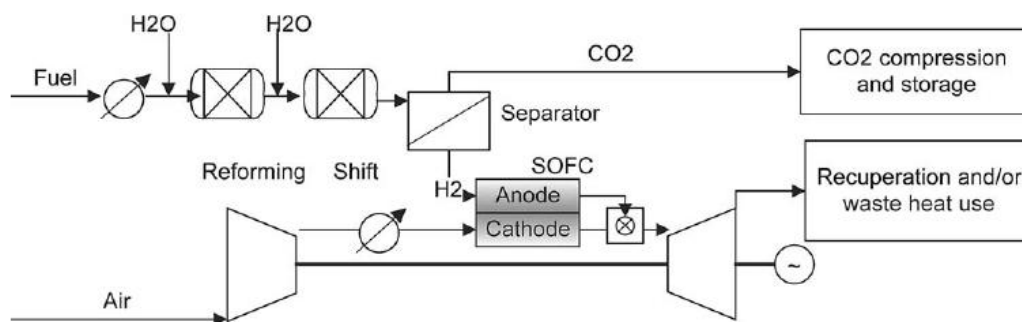


Figure 9: SOFC-GT with pre-fuel cell CO<sub>2</sub> capture [1.20]

The basic concept of post-fuel cell CO<sub>2</sub> capture is shown in Fig. 10. The anode off-gas has a high CO<sub>2</sub> content, but also contains H<sub>2</sub>O, CO and H<sub>2</sub>. The water can easily be removed by conventional techniques (cooling, knock-out, additional drying). Oxidizing the H<sub>2</sub> and CO from the SOFC anode with air will result in a high dilution of the stream with nitrogen.

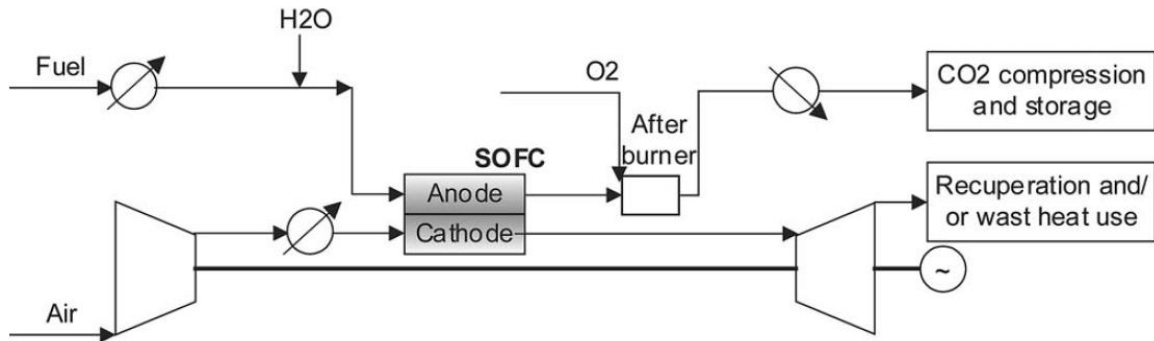


Figure 10: SOFC-GT with post-fuel cell hydrogen oxidation [1.20]

To avoid dilution with nitrogen pure oxygen can be used for oxidation, but this will probably result in significant additional costs and energy consumption if oxygen is not available. In the system used for the project an air separation unit and thus the oxygen for oxy-combustion is available. In case no oxygen is available the use of an oxygen-conducting membrane reactor (OCM-reactor), placed after the SOFC, could be integrated into the scheme (figure 11). The anode off-gas is fed to one side of the membrane while the cathode off-gas is fed to the other side of the membrane. The membrane is selective to oxygen, which permeates from the cathode off-gas stream to the anode off-gas. In the membrane unit, H<sub>2</sub> and CO are oxidized. The retentate of the membrane unit consists of CO<sub>2</sub> and water. The water can be removed using conventional techniques.

There is almost no need for after treatment of the CO<sub>2</sub> rich stream, only compression for storage. Both of these concepts, oxy-combustion and the oxygen conducting membrane, are investigated in the next chapters. The exact configuration is yet to be decided due to the fact that the exact configuration depends on how the membrane can be integrated into the system.

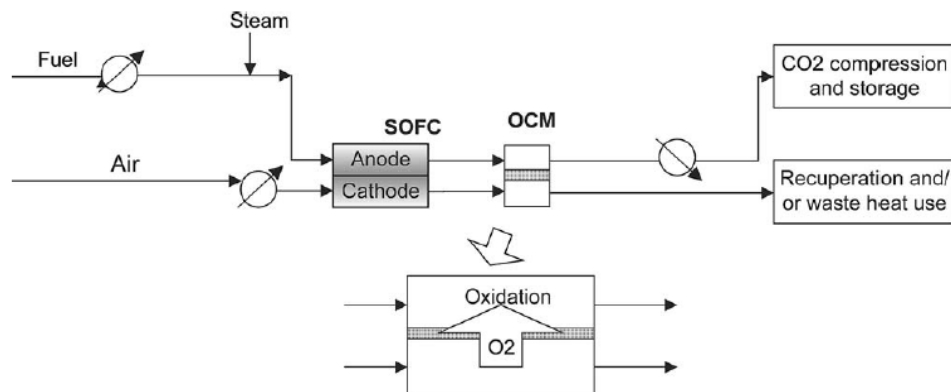


Figure 11: SOFC-GT with OCM-afterburner [1.20]

Another concept for CO<sub>2</sub> capture in SOFC and hybrid systems uses a water-gas shift membrane reactor afterburner (WGSMR-afterburner). The working principle is shown in figure 12. Air is fed to the SOFC cathode and fuel is fed to the SOFC anode. The cathode off-gas is fed to the permeate side of the membrane reactor and the anode off-gas is fed to the feed side of the membrane reactor. On the feed side the water-gas shift reaction takes place producing H<sub>2</sub> and CO<sub>2</sub>. The H<sub>2</sub> permeates through the hydrogen selective membrane in the WGSMR-afterburner. On the permeate side this hydrogen is burned with O<sub>2</sub> present in the SOFC cathode off-gas. This results in a very low hydrogen partial pressure on the permeate side, thus resulting in a high H<sub>2</sub> permeation rate.

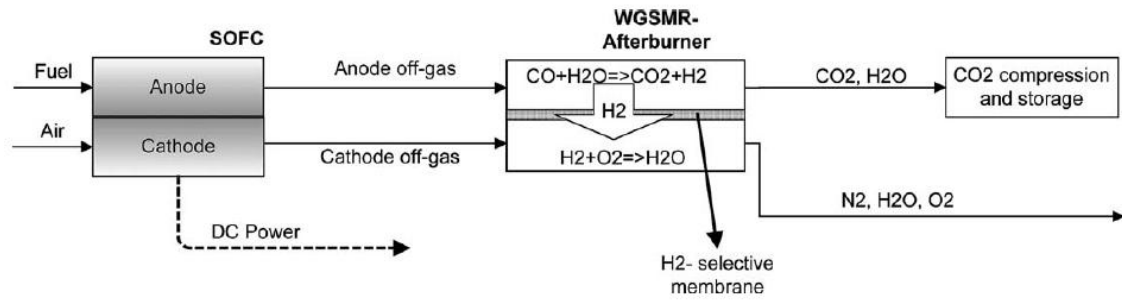


Figure 12: Working principle of the WGSMT-afterburner [1.20]

The WGSMT-feed side products are  $\text{CO}_2$  and  $\text{H}_2\text{O}$ , and small amounts of  $\text{H}_2$  and  $\text{CO}$ , which can be removed by (catalytic) oxidation with air resulting in only a small dilution with nitrogen. The water can be removed easily e.g. with cooling. The resulting  $\text{CO}_2$  can be used for sequestration without the need for further treatment. The WGSMT permeate side products are  $\text{N}_2$ ,  $\text{H}_2\text{O}$  and  $\text{O}_2$ .

The WGSMT concept has the same advantages as the OCM-afterburner concept. A pure  $\text{CO}_2$  stream is available after water knock-out, without the requirement of large, complex and steam-consuming  $\text{CO}_2$  scrubbing equipment. Thus, the system offers the prospect for power production with  $\text{CO}_2$  capture. Moreover, the system has some additional advantages above the OCM-afterburner concept:

- The flux through the membrane is towards the gas turbine side. Thus, the mass flow through the expander is increased (higher power production), and the dilution of  $\text{CO}_2$  with water is decreased.
- With the projected membrane materials higher fluxes may be achieved without the necessity for imposing a current on the membrane material as might be required with OCM membranes.

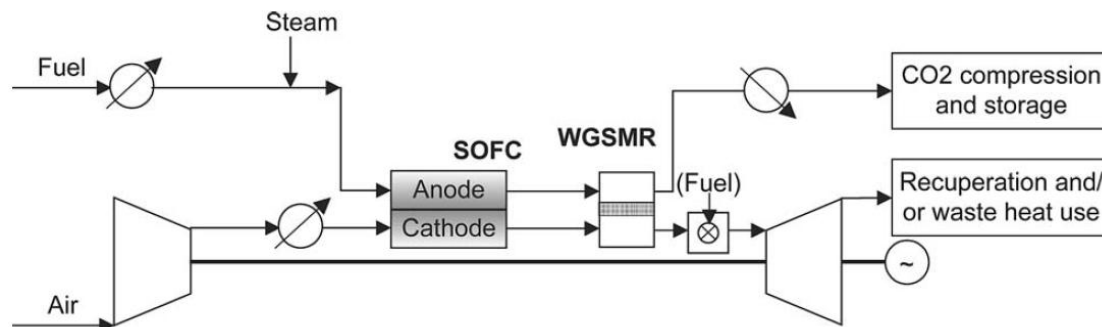


Figure 13: Hybrid cycle with WGSMT-afterburner [1.20]

The pressurized hybrid cycle with a WGSMT-afterburner is shown on figure 13. Air is fed to the gas turbine compressor, heated and fed to the SOFC cathode. Fuel is heated, mixed with steam and fed to the SOFC anode. The anode off-gas is fed to the feed side of the WGSMT. Cathode off-gas is used as a sweep gas for the permeate side of the WGSMT. The retentate stream from the WGSMT-afterburner is cooled and flows to the  $\text{CO}_2$  compression and storage section. The permeate stream from the WGSMT-afterburner passes an optional combustion chamber for additional firing to increase the temperature at the gas turbine inlet. It is then expanded in the gas turbine. The additional combustion of fuel will completely remove emissions of  $\text{CO}_2$ , but compared to just venting the  $\text{CO}_2$ , the amount vented in this

case is relatively small. The concept with additional combustion of fuel is not a subject of this thesis report. But two concepts using a  $H_2$ -conducting membrane are investigated, one with  $N_2$  as sweep gas and the other with air as sweep gas.

## 1.7 Membrane technologies

Membranes are devices which offer the possibility of selectively remove some species from a gas mixture. There are porous membranes where entire molecules pass through the membrane. This allows easier permeation but has a negative effect on selectivity. Solid (metallic) membranes offer very high selectivity but the permeation rates are much lower due to the fact that atomic permeation takes place and this involves numerous processes like those seen in figure 14.

In this thesis report two kinds of membranes were used:

- $H_2$ -conducting membrane (Palladium based membrane)
- $O_2$ -conducting membrane (Perovskite based membrane)

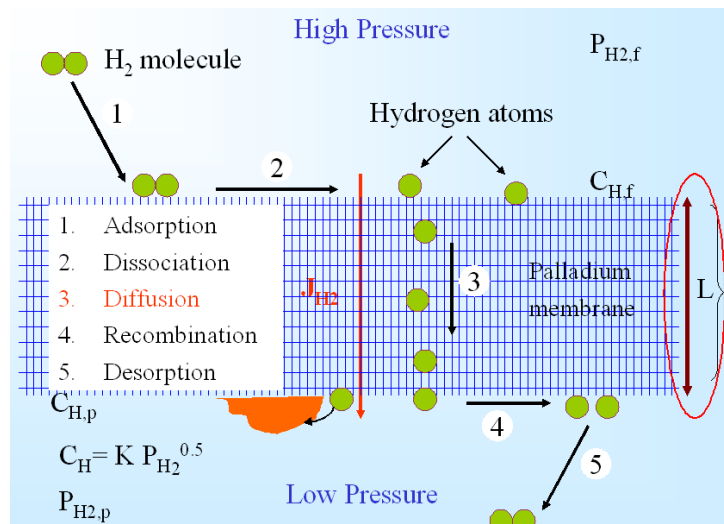


Figure 14: Hydrogen transport through Pd membranes [1.21]

The  $H_2$ -membrane has more emphasis here because of the reason the membrane is used in the first place: to withdraw as much  $H_2$  from the depleted anode side as possible. Using membranes does not allow removing all the  $H_2$  from the retentate side, because the partial pressure difference of the species on each side is the driving force for the permeation process.

## 1.8 Aspen Plus [1.22]

### *Conceptual design of chemical processes*

Aspen Plus is a market-leading process modeling tool for conceptual design, optimization, and performance monitoring for the chemical, polymer, specialty chemical, metals and minerals, and coal power industries. Aspen Plus is a core element of AspenTech's aspenONE™ Process Engineering applications.

## Features

- **Efficient workflow** for process design, equipment sizing, and preliminary cost estimation within one environment through integration with other aspenONE Process Engineering tools including Aspen Process Economic Analyzer cost modeling software and Aspen HTFS+® heat exchanger design tools.
- **Online deployment of models** as part of an open-loop operator advisory system or in closed-loop, real-time optimization/advanced process control applications when used with Aspen Online Deployment™ and Aspen Simulation Workbook™.
- **Unique equation-oriented architecture.** Aspen Plus's unique combination of sequential-modular and equation-oriented solution technologies facilitates the simulation of wide-scale, integrated chemical processes.
- **Best-in-class physical properties methods and data.** Aspen Plus includes extensive databases of pure component and phase equilibrium data for conventional chemicals, electrolytes, solids, and polymers. Ongoing collaboration with the U.S. National Institute of Standards and Technology ensures easy access to the best available experimental data and methods.
- **Comprehensive library of unit operation models** to address a wide range of solid, liquid, and gas processing equipment. The open architecture lets you build your own libraries of unit operation models with Aspen Custom Modeler® or programming languages. CAPE-OPEN compliant models can also be used with Aspen Plus.
- **Workflow automation.** Aspen Plus models can be linked to Microsoft Excel® using Aspen Simulation Workbook or Visual Basic® and used to automate the engineering workflow and deploy the model to a wider range of end users in the field.
- **Links to third-party tools.** Aspen Plus includes links to several well-known tools including the OLI's electrolyte package and Technip's SPYRO ethylene cracker models.

## Options

A number of optional extensions are available to enhance the value of Aspen Plus:

- **Aspen Plus Dynamics®** is used for safety and controllability studies, sizing relief valves, optimizing transition, start-up, and shutdown policies.
- **Aspen Rate-Based Distillation** improves the rigor and accuracy of the distillation models using proven rate-based technology.
- **Aspen Batch Distillation** is a dynamic batch distillation modeling tool that can be run stand-alone or inside an Aspen Plus flow sheet.
- **Aspen Polymers Plus®** extends Aspen Plus with a complete set of polymer thermodynamics methods and data, rate-based polymerization reaction models, and a library of industrial process models.
- **Aspen Distillation Synthesis** is used for the conceptual design of distillation schemes for separation of mixtures with non-ideal vapour liquid equilibrium behaviour.

## Benefits

Aspen Plus is a proven, industry-standard solution with over twenty years of use in the field. Customers have recognized and reported:

- Up to \$15M per year in incremental profitability from process optimization



- Up to \$10M per year in capital savings resulting from improved designs
- Up to \$1M per year of reduced labour costs from improved conceptual engineering workflow

## 1.9 Objectives

Several CO<sub>2</sub> capture system concepts can be integrated with fuel cell systems, but the selection of one over another requires detailed study of long-term technical and economic performance [1.23].

The primary objectives of the present study can be viewed as answering the following questions through the modeling and simulation of various SOFC tail-gas configurations:

- 1) How do different tail-gas concept configurations affect mass flows?
- 2) Where and how much heat is needed for heating/cooling the gas streams?
- 3) Is it necessary to use any external heat sinks for heating/cooling of the gas streams?
- 4) Comparing the net energy production of the modeled systems and the breakdown of where and how much energy is produced and consumed.
- 5) How much of the cathode flow should be recycled to have the needed air temperature at the cathode inlet?
- 6) Is it necessary to vary the air flow going to the cathode of the SOFC with different tail-gas processing concepts (fraction of air recycled)?
- 7) What effect does the increased/decreased flow of air have on the net-power produced (more power to compress the air, more power produced by the gas turbine due to the increased mass flow)?

## 1.10 Methodology

The research methodology for the present study was carried out in the steps listed below. In practice, the sequence of the steps did not occur in the exact order presented below. Instead, some of them occurred simultaneously and some of the later steps were done earlier [1.23].

- 1) To find from the literature the content and parameters of syngas after the cleanup processes
- 2) To develop a fuel cell (SOFC) model using components available in Aspen Plus
- 3) If possible validate the SOFC model with an existing model
- 4) Find out how membranes work, what are the driving forces of permeation
- 5) Model the membrane function in an Excel spreadsheet and then connect it with Aspen Plus, importing the parameters and content of gas streams from aspen and then export the results back to Aspen Plus
- 6) Development of different tail-gas concepts
- 7) Calculating the parasitic losses (compression of air/CO<sub>2</sub>, water knock-out from CO<sub>2</sub>, compression permeate streams etc) and power produced in the system
- 8) Calculate the overall efficiencies of the different concepts, using the higher and lower heating value of the coal fed to the gasifier, with and without CO<sub>2</sub> capture

- 9) Compare the efficiencies of the different concepts with each other and with just mixing the cathode and anode streams, where CO<sub>2</sub> is vented
- 10) Analyze the results and discuss why the results occurred
- 11) Possible suggestions as to what could be done to improve the performance of different concepts or some parts of them

The goal of the modeling is to provide a sufficiently realistic model which is able to meet the research objectives and answer questions like:

- How much power was generated and consumed by the whole system?
- How to demonstrate the chemical reactions taking place in the fuel cell?
- What were the temperature changes of reactant flows?
- How much is the mass transfer from the cathode side to the anode side and how much power was produced by the SOFC?
- How much heat is produced in the tail-gas from combusting the fuel not reacted in the SOFC?
- How does mass transfer between the depleted anode and cathode streams?
- How does heat change between the anode and cathode streams take place?

To meet the objectives, all components in the system have the ability to predict performance at a steady state. It is also apparent that different levels of modeling will be required to simulate different parts of the system. For example, the H<sub>2</sub>-conducting membrane model is capable of resolving the distribution of composition (H<sub>2</sub> molar flow and partial pressure) of the gas stream along the length of the membrane (one-dimensional) while simulation of other equipment employs relatively simple (zero-dimensional) steady-state thermodynamic models.

In order to maintain focus on the research objectives, the scope of the project was limited by an analysis of the systems using the same amount and content of syngas and air fed to the system. The only parts that were changed were the tail-gas processing and CO<sub>2</sub> separation concepts.

## 1.11 Chapter References

- 1.1 <http://www.eia.doe.gov/oiaf/ieo/coal.htm> - Web-page
- 1.2 <http://www.eia.doe.gov/oiaf/ieo/ieorefcase.html> - Excel-file (Table A2)
- 1.3 <http://www.eia.doe.gov/cneaf/coal/page/acr/table26.html> - Web-page
- 1.4 [http://en.wikipedia.org/wiki/Fossil\\_fuel\\_power\\_plant](http://en.wikipedia.org/wiki/Fossil_fuel_power_plant) - Web-page
- 1.5 U.S. Department of Energy (2002) *Final Report: Major environmental aspects of gasification-based power generation technologies*. U.S. Department of Energy, Office of Fossil Energy, National Energy Technology Laboratory.
- 1.6 Bredesen, Jordal, Bolland, *High-temperature membranes in power generation with CO<sub>2</sub> capture*. Chemical Engineering and Processing 43 (2004) 1129-1158
- 1.7 <http://www.parl.gc.ca/information/library/PRBpubs/prb0704-e.htm#future> – web page
- 1.8 [http://www.netl.doe.gov/technologies/coalpower/cctc/summaries/pinon/images/pinon\\_schematic.jpg](http://www.netl.doe.gov/technologies/coalpower/cctc/summaries/pinon/images/pinon_schematic.jpg) - web page

- 1.9 <http://en.wikipedia.org/wiki/Gasification> - web page
- 1.10 [http://en.wikipedia.org/wiki/Carbon\\_tax](http://en.wikipedia.org/wiki/Carbon_tax) - web page
- 1.11 Stiegel, Maxwell, *Gasification technologies: the path to clean, affordable energy in the 21<sup>st</sup> century*, Fuel Processing Technology 71 (2001) 79-97
- 1.12 U.S. Department of Energy (2004) *Fuel Cell Handbook (Seventh Edition)*. U.S. Department of Energy, Office of Fossil Energy, National Energy Technology Laboratory.
- 1.13 Dr. Neal Sullivan (2008), *FC 602: Types of Fuel Cells*, Neal Sullivan, RES FC602
- 1.14 O'Hayre, Cha, Colella, Prinz, *Fuel Cell Fundamentals*, John Wiley & Sons (2006)
- 1.15 [http://en.wikipedia.org/wiki/Brayton\\_cycle](http://en.wikipedia.org/wiki/Brayton_cycle) - web page
- 1.16 <http://www.grc.nasa.gov/WWW/K-12/airplane/Images/braytonts.gif> - web page
- 1.17 [www.chrisbence.com/.../braytoncycle.jpg](http://www.chrisbence.com/.../braytoncycle.jpg) web page
- 1.18 [www.taftan.com/thermodynamics/PLANT1.GIF](http://www.taftan.com/thermodynamics/PLANT1.GIF) - web page
- 1.19 <http://www.mhlt.uwaterloo.ca/courses/me354/lectures/pdf/c8.pdf> - web page
- 1.20 Djikstra, Jansen, *Novel concepts for CO<sub>2</sub> capture*. Energy 29 (2004) 1249-1257
- 1.21 Al Raisi, Gardner, *Surface and fluid phase transport effects on hydrogen permeability through palladium-based membranes*, AIChE Annual Meeting, Salt Lake City, Utah, November 2007
- 1.22 <http://www.aspentech.com> – web page
- 1.23 R.J. Braun, *Optimal design and operation of solid oxide fuel cell systems for small-scale stationary applications*, Ph.D. Thesis, University of Wisconsin-Madison (2002)

## 2 Modeling of various CO<sub>2</sub> capture strategies in the SOFC-gas turbine subsystem

Modeling of fuel cells systems can proceed at numerous levels of detail ranging from stack design levels to overall systems levels. As this project is concerned with sub-system design of an IGFC, the level of modeling detail required for most system components is more general and will not be too detailed (overall mass and energy balances and incorporation of component performance characteristics). In addition, in the beginning no SOFC model was available and what was done to simulate the fuel cell in the system is described later in this chapter. The created SOFC model was verified using an existing SOFC model from NETL.

In this chapter, an overview of the approach for modeling an IGFC-GT with different tail-gas processing concepts is presented. The associated assumptions and modeling simplifications are then discussed. The following was modeled:

- A fuel cell model
- A membrane model
- The incorporation of the membrane model to the system
- The Brayton and Rankine cycles
- CO<sub>2</sub> preparation for storage

On Fig. 15 the IGFC system configuration with the baseline tail-gas concept (oxy-combustion) can be seen. In this work only a part of this system is modeled (SOFC-GT, CO<sub>2</sub> separation, and preparation for sequestration).

For the baseline configuration oxy-combustion of tail-gas has been chosen. This choice is based on the fact that this technology is already commercially available and in addition there is already an air separation unit (ASU) for producing oxygen for the gasifier in this system, and for it to supply oxygen for the oxy-combustion is a question of sizing the ASU. The additional energy needed to compress additional air and for separating extra O<sub>2</sub> has to be taken into consideration.

For comparison three other concepts are being modeled, these are:

1. Tail-gas combustor without CO<sub>2</sub> capture, where the CO<sub>2</sub> is being vented
2. Water-gas shift (H<sub>2</sub>-conducting) membrane reactor (WGSMR)
  - a. Nitrogen as sweep gas
  - b. Air as sweep gas
3. O<sub>2</sub>-conducting membrane reactor

All these concepts alter the system configuration of the mass flows and thermal integration. Possible examples of these configurations; oxy-combustion, H<sub>2</sub> and O<sub>2</sub> conducting membranes reactors, can be seen in chapter 1 (Fig. 10-13).

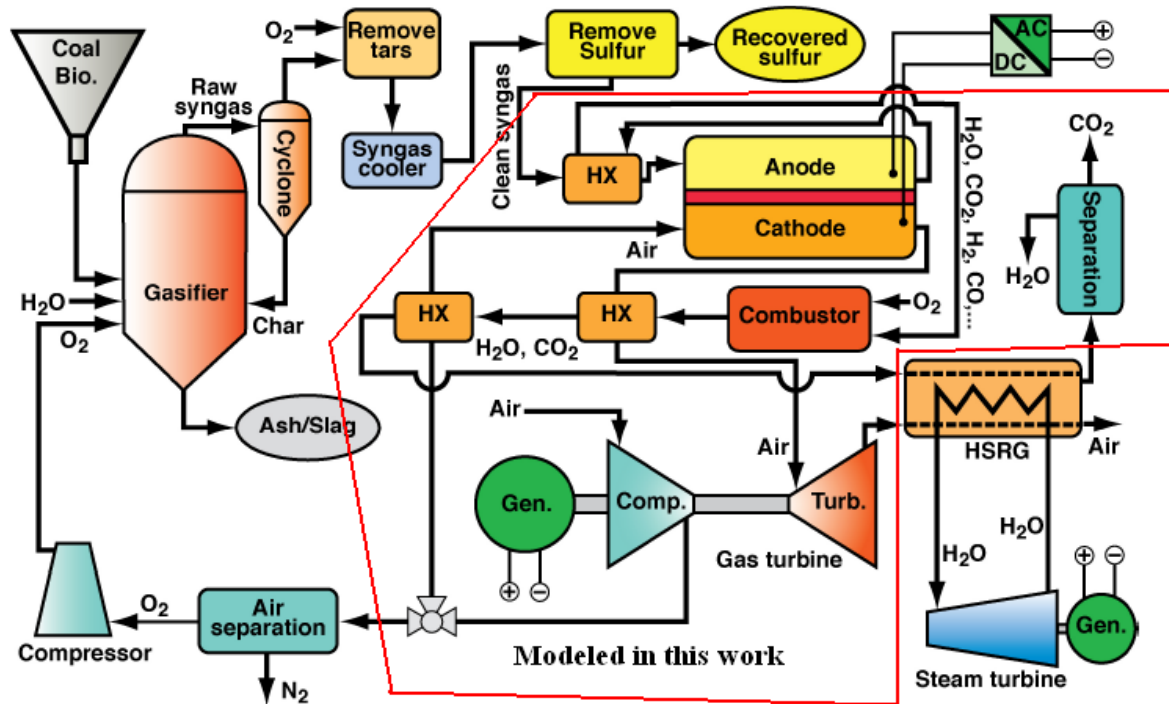


Figure 15: Baseline IGFC System Configuration [2.1]

The gas turbine in Fig. 15 produces power but also compresses air for the cathode of the SOFC. In addition some air goes to the air separation unit (ASU). The ASU provides oxygen for the gasifier and also for the oxy-combustor.

In the gasifier the coal slurry is turned into a synthetic gas (syngas), consisting mainly of CO and H<sub>2</sub>. Before entering the anode of the fuel cell the char, tar and sulphur have to be removed from the syngas. The CO is shifted to H<sub>2</sub> and CO<sub>2</sub> in the cathode side and around 80% of the H<sub>2</sub> content in the syngas is reacted electrochemically with O<sub>2</sub>. There are two main reasons for not reacting all of the H<sub>2</sub> in the syngas:

1. To maintain a sufficient rate of reaction in the end of the fuel cell
2. To be able to increase the temperature of the depleted syngas by combusting the fuel (H<sub>2</sub>, CO and some CH<sub>4</sub>) left in the depleted syngas

After combusting the fuel residues in the syngas, the heat created is transferred to the cathode stream exiting the SOFC. In addition the anode stream is used to pre-heat the air stream entering the cathode and if possible additional heat is utilized in the heat recovery steam generator (HSRG). After these processes water knock-out and compressing of the anode stream takes place, and after that the content of the anode stream should be almost entirely made up of CO<sub>2</sub>.

## 2.1 SOFC modeling

An SOFC model was created using elements available in Aspen Plus 2006. The following processes had to be taken into account:

1. Pre-heating of the reactant streams
2. Chemical reactions (electrochemical “burning” of  $H_2$ , shifting of  $CO$  and  $CH_4$ )
3. Fuel utilization
4. Changes in mass flows
5. Temperature changes of the reactant flows
6. Power generated by the SOFC

The fuel cell model is presented on Fig. 16. The fuel cell itself is surrounded by the red line. In addition the pre-heater of the anode stream and the recycling loop of the cathode stream can be seen.

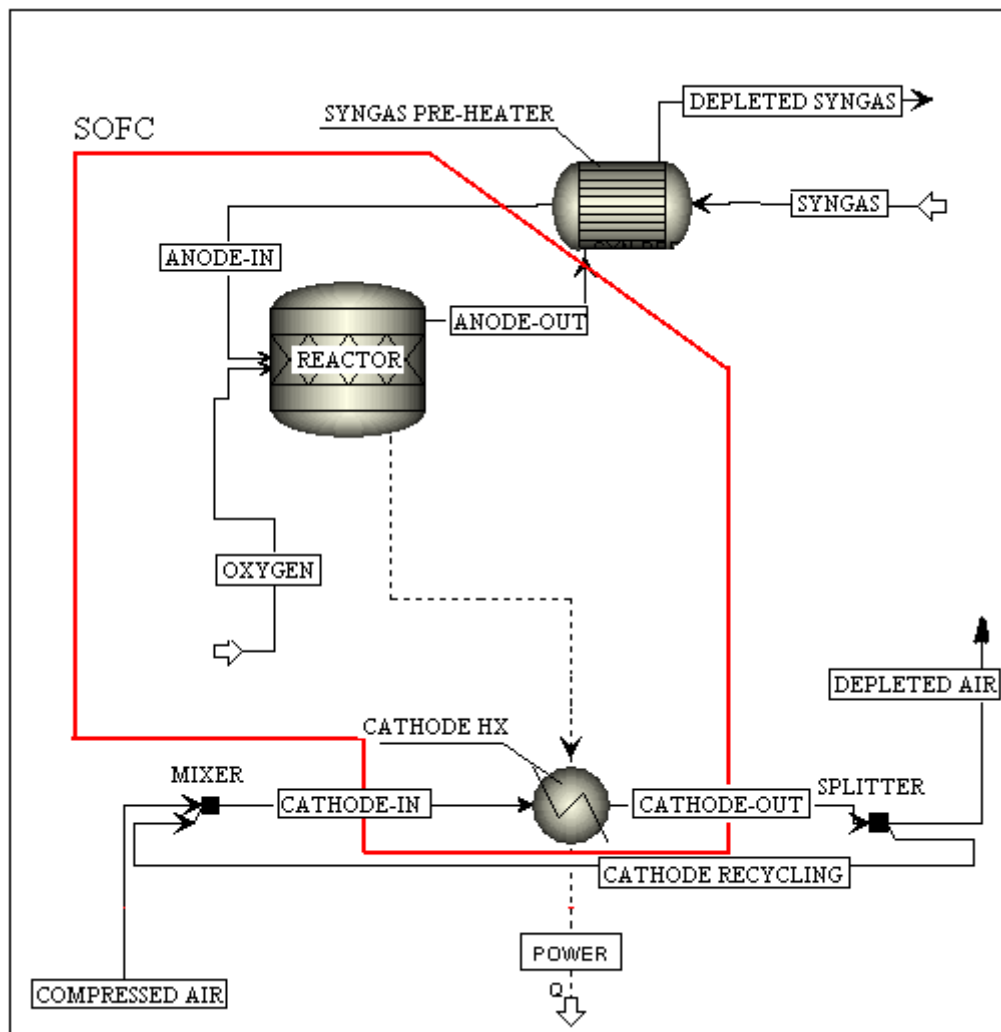


Figure 16: Fuel Cell model in Aspen Plus

The reactant streams have to be at  $650^{\circ}\text{C}$  when entering the fuel cell. The syngas can be heated to  $650^{\circ}\text{C}$  using the anode-out stream, which is at  $750^{\circ}\text{C}$ . For the cathode stream a different approach was chosen: the recycling of the cathode stream, which is at  $800^{\circ}\text{C}$  on the outlet of the cathode. The split fraction needed to be recycled depends on the temperature of the compressed air before the recycling loop.

Two chemical reactions were simulated using a stoichiometric reactor (the stoichiometric reactor allows determining which reactions take place and what is the fractional conversion of the species). In figure 17 the reactions are presented. As can be seen the reactions no. 1 and 4 are identical. The reason for reacting  $H_2$  with  $O_2$  twice can be explained like this: if reaction no. 1 is discarded, some of the CO and  $CH_4$  will not be shifted because there is not sufficient water available to conduct these reactions. And if reaction no. 4 is left aside the amount of  $H_2$  produced during the water-gas shift reaction will not be reacted and the desired fuel utilization is not achieved. It is also important to indicate that the reactions have to occur in sequence (like seen in Fig. 17). The fractional conversion for  $H_2$  is 1 in both reactions and 0,8 for CO and  $CH_4$ . These numbers do not determine the fuel utilization in the fuel cell. The reason for this is explained further on in this chapter.

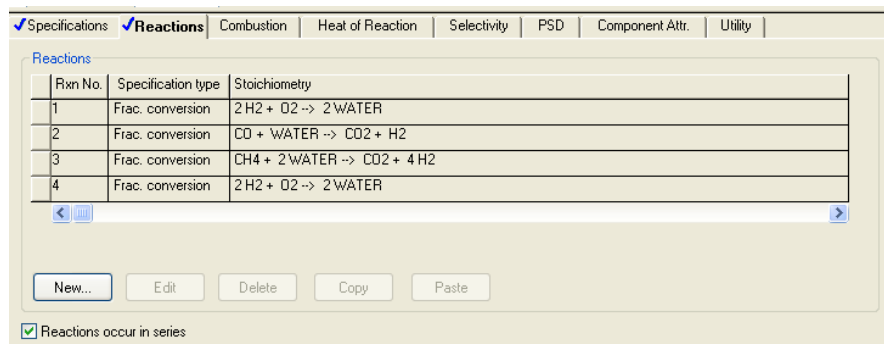


Figure 17: Reactions in the Stoichiometric reactor (Aspen Plus)

Syngas and pure oxygen are fed to the reactor. The operating conditions of the reactor were set as seen on Fig. 18. The operating temperature that was set is important because then the heat duty of the reactions in the reactor can be calculated. The total heat duty of the reactions heats up the anode stream to  $750^\circ C$  (in the reactor element) and the cathode stream to  $800^\circ C$  (in the cathode HX). What is left is the heat duty, or “POWER”. Later this heat duty (“POWER”) can be used to determine the right mass flow of air into the SOFC cathode by comparing the heat duty (“POWER”) with the  $P_{DC}$  produced in the SOFC.

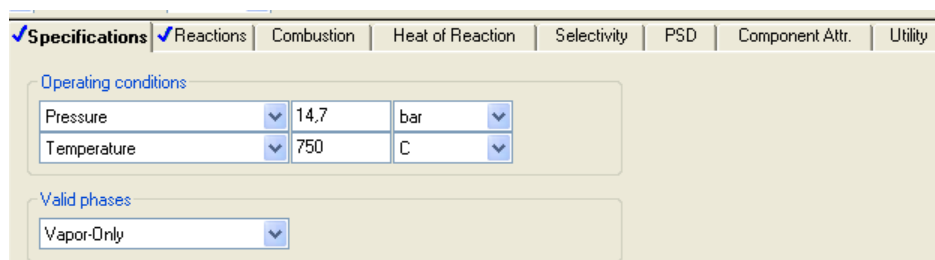


Figure 18: Specifications of the Stoichiometric reactor (Aspen Plus)

In addition, the reactions and the reaction fractions of species in the reactor have to be determined. This is done in the reactor setup → reactions, as seen in Fig. 17. Here  $H_2$  reacts with  $O_2$ ; CO and  $CH_4$  are shifted to  $CO_2$  and  $H_2$  by reacting them with  $H_2O$ . Although the water-gas shift reaction may go to the reactants side at higher temperatures (reverse water-gas shift reaction), the fact that  $H_2$ , one of the products, is constantly withdrawn from the anode side causes an electrochemical reaction with  $O_2$  and the reaction is shifted to the product side.

The fuel utilization was determined by the molar flow of oxygen flowing to the reactor. To control the fuel utilization and the oxygen going through the electrolyte of the fuel cell a user

defined model was created. The user defined model can be in FORTRAN or an Excel spreadsheet. An Excel spreadsheet was used for this model.

The input parameters to the spreadsheet are:

- Content of syngas entering the SOFC anode
- Content and temperature of air entering the SOFC cathode
- Temperature of air at the SOFC cathode outlet

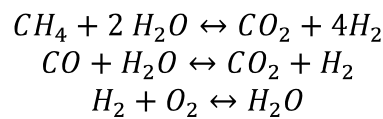
and the returns used the following calculated parameters:

- Content and flow of the air exiting the SOFC cathode
- Flow and temperature of oxygen entering the reactor

The temperature of the oxygen flow to the reactor is calculated with the following formula:

$$T_{OXYGEN} = (T_{AIR-FC1} + T_{AIR-FC2})/2 \quad [^{\circ}C]$$

The flow of pure oxygen into the reactor takes into account the hydrogen content (including how much can be produced from CO and CH<sub>4</sub>) in the syngas and oxidizes the desired amount. Parallel to the oxidation of H<sub>2</sub>, the shifting of CH<sub>4</sub> (the CH<sub>4</sub> is assumed to be shifted directly to CO<sub>2</sub> and H<sub>2</sub>) and CO takes place. In this research the fuel utilization was chosen to be 80%.



According to the chemical reactions shown, one mole of CH<sub>4</sub> can produce four moles of H<sub>2</sub>; and to oxidize four moles of H<sub>2</sub>, two moles of O<sub>2</sub> is needed. One mole of CO can produce one mole of H<sub>2</sub>. So to oxidize one mole of H<sub>2</sub>, half a mole of O<sub>2</sub> is needed. Taking this into account the formula for the molar flow of oxygen to the reactor is:

$$\dot{v}_{OXYGEN} = \left( 2 \times \dot{v}_{SYNGAS2}^{CH_4} + \left( \dot{v}_{SYNGAS2}^{CO} + \dot{v}_{SYNGAS2}^{H_2} \right) / 2 \right) \times U_F \quad [kmol/hr]$$

Where the U<sub>F</sub> is the fuel utilization and this is determined by the user in the Excel spreadsheet. The user defined fuel utilization is valid even if the reaction fractions for all the reactions in the reactor are 1. This is because the Excel sheet will overwrite the molar flow of pure oxygen to the reactor and this will be only as much as needed for oxidation of the fraction of fuel determined by the user.

To have a mass balance on the cathode side the molar flow of oxygen in the outlet of the cathode must be smaller than in the inlet by the amount fed to the reactor. The mass balance is provided by the following relations:

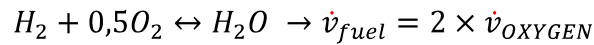
$$\begin{aligned} \dot{v}_{AIR-FC2}^{N_2} &= \dot{v}_{AIR-FC1}^{N_2} \quad [kmol/hr] \\ \dot{v}_{AIR-FC2}^{O_2} &= \dot{v}_{AIR-FC1}^{O_2} - \dot{v}_{OXYGEN} \quad [kmol/hr] \\ \dot{v}_{AIR-FC2} &= \dot{v}_{AIR-FC1} - \dot{v}_{OXYGEN} = \dot{v}_{AIR-FC2}^{N_2} + \dot{v}_{AIR-FC2}^{O_2} \quad [kmol/hr] \end{aligned}$$



To get the power output of the SOFC the following formula was used:

$$\dot{v}_{fuel} = \frac{i}{nF} \rightarrow i = \dot{v}_{fuel} \times nF \text{ [A]}$$

Where the  $\dot{v}_{fuel}$  is the molar flow of fuel reacted in the fuel cell [mol/s],  $i$  is the current produced by the electrochemical reaction [A],  $n$  is the number of electrons released during the reaction and  $F$  is the Faradays constant  $F=96485 \text{ C/mol}$ . The  $\dot{v}_{fuel}$  was calculated through the oxygen flow to the reactor using the following relationship:



Power output calculations:

$$P = i \times V \text{ [W]}$$

Where the  $V$  is the cell voltage, which was chosen to be 0,7V.

The calculated DC power of the SOFC should be equal to heat duty “POWER” (Figure 18).

$$P_{in} = P_{DC} + \Delta Q_{AIR} + \Delta Q_{SYNGAS}$$

$$\Delta Q_{AIR} = m_{AIR} \times c_p^{AIR} \times \Delta T$$

Where  $P_{in}$  is the power input of  $H_2$  (including  $H_2$ , which could be produced by shifting all the CO and  $CH_4$ ) in syngas reacted [kW];  $P_{DC}$  is the DC power generated by the SOFC [kW];  $\Delta Q_{AIR}$  is the heat duty to increase the temperature of air from 650°C to 800°C [kW];  $\Delta Q_{SYNGAS}$  is the heat duty to increase the temperature of syngas from 650°C to 750°C [kW];  $m_{AIR}$  is the mass flow of air [kg/s];  $c_p^{AIR}$  is the heat needed to increase the temperature of 1 kg of air 1 by degree [kJ/(kg°C)];  $\Delta T$  is the temperature change caused by adding or removing heat [°C].

For  $P_{DC}$  to be equal to the heat duty in stream “POWER” only the heat added to the air stream ( $\Delta Q_{AIR}$ ) can be changed,  $P_{DC}$  is constant and also the heat added to the syngas is limited because the content, flow rate and temperature change are constant.

The mass flow of air is adjusted in such a way that the  $Q_{POWER}$  will be equal to  $P_{DC}$ :

$$Q_{POWER}(m_{AIR}) = P_{DC}$$

This assumption is based on the first law of thermodynamics which is the law of conservation of energy (The increase in the internal energy of a system is equal to the amount of energy added by heating the system, minus the amount lost as a result of the work done by the system on its surroundings) [1.26].

## 2.2 SOFC model verification

To verify the created SOFC model an SOFC model, operating at 1 bar, created in the National Energy Technology Laboratory (NETL) was available. The principals of the two models were similar but in the NETLS model instead of the cathode the anode stream was recycled.

To compare these two models the data from between the recycling loop was taken, that way the recycling does not have any effect on the results, this is being illustrated in Fig. 19. This was also done with the anode streams of the NETL SOFC model. Both models have a fuel utilization of 80%.

The inlet pressure of the reactants was increased from 1 bar to 15,1 bars. Then the NETL model was run. The syngas content was taken from between the anode recycling loop and the anode inlet of the NETL SOFC model. Also the air content and parameters were taken from the NETL model; this is because the NETL model adjusts the air flow in a way that the heat duty “POWER” (Figure 19) is equal to the calculated direct current (DC) power.

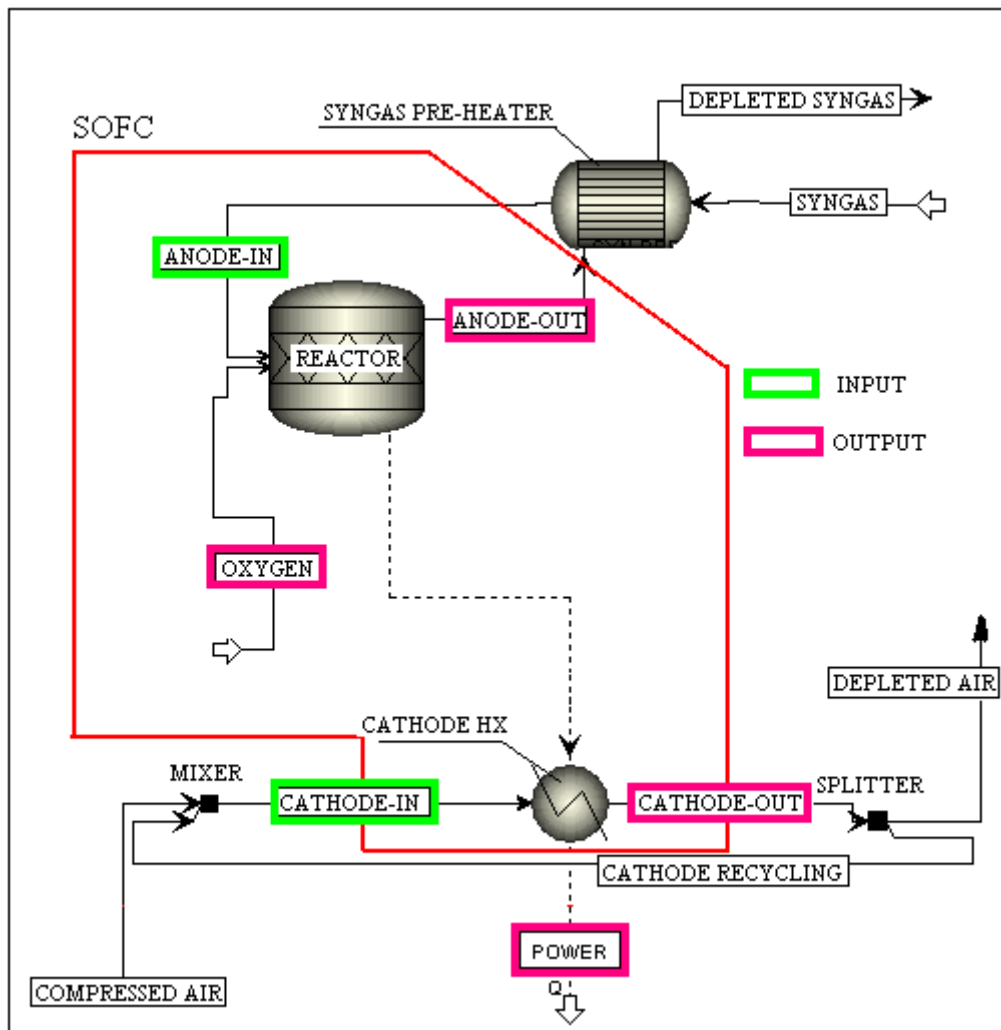


Figure 19: Fuel Cell model in Aspen Plus

On table 6 the inputs and outputs of the SOFC models are presented:

	Anode inlet	Anode outlet (NETL)	Anode outlet
Mole flow [kmol/hr]	14818	14836	14832
Temperature [°C]	649	750	750

Pressure [bar]	15	15	15
CH <sub>4</sub>	8,8	0,02	1,7
CO	1454	257	290
CO <sub>2</sub>	6235	7440	7406
H <sub>2</sub>	1295	298	259
H <sub>2</sub> O	5604	6617	6654
N <sub>2</sub>	221	221	221
O <sub>2</sub>	-	-	-

*Table 6: Input and comparison of anode outputs of the two SOFC models*

As seen in table 6, if both of the syngas have the same content and other parameters of the inlet of the anode the outlet is also almost the same; only slight variation is noticed. The H<sub>2</sub> left in the anode stream (including in CO and CH<sub>4</sub>) is the same.

	Cathode inlet	Cathode outlet (NETL)	Cathode outlet
Mole flow [kmol/hr]	37939	36825	36825
Temperature [°C]	650	800	800
Pressure [bar]	15	15	15
Oxygen flow [kmol/hr]		1113	1113

*Table 7: Flows of the cathode*

	NETL SOFC model	SOFC model
Heat duty of reactor [Gcal/hr]	124	125
Heat duty of SOFC [Gcal/hr]	81	80
Heat duty of cathode [Gcal/hr]	43	45
P <sub>DC</sub> of SOFC [kW]	94241	83819

*Table 8: Heat duties and P<sub>DC</sub>*

As seen in table 8, and also in all the previous tables, all the results are comparable and only slight differences are noticeable, except for the P<sub>DC</sub> of the SOFC's. The reason for this may be the selected cell voltage. For the current model it was chosen to be 0,7 V. To make these powers equal the cell voltage has to be 0,797 V. To make sure that the cell voltage does not change, the flow of syngas was varied. In all cases the power outputs (P<sub>DC</sub>) of the two SOFC models were equal if the cell voltage the SOFC model created was 0,787 V.

The comparison of the two SOFC models showed that the one created has the same performance as the one from NETL. Except that the P<sub>DC</sub> generated were different, in order to get equal power outputs the cell voltage has to be 0,79 V; which, compared to the cell voltage usually used, 0,7 V, is relatively high. To have a compromise the average value of these two was chosen to be – 0,745 V.

## 2.3 Modeling of air compression

In the IGFC system compressed air needs to be supplied to two places: the air separation unit (ASU), which supplies pure oxygen for the gasifier, and the cathode of the pressurized

SOFC. For this there is only one compressor, and to supply this compressed air to two places a splitter was used to split the stream into two, where the split fraction of air going to the ASU was set to be 0,1667 and the split fraction of air heading to the cathode of the SOFC is 0,8333. These split fractions are subject to change according to how much air needs to be supplied to the ASU (Oxygen for the gasifier and the oxy-combustion) and to the cathode of the SOFC.

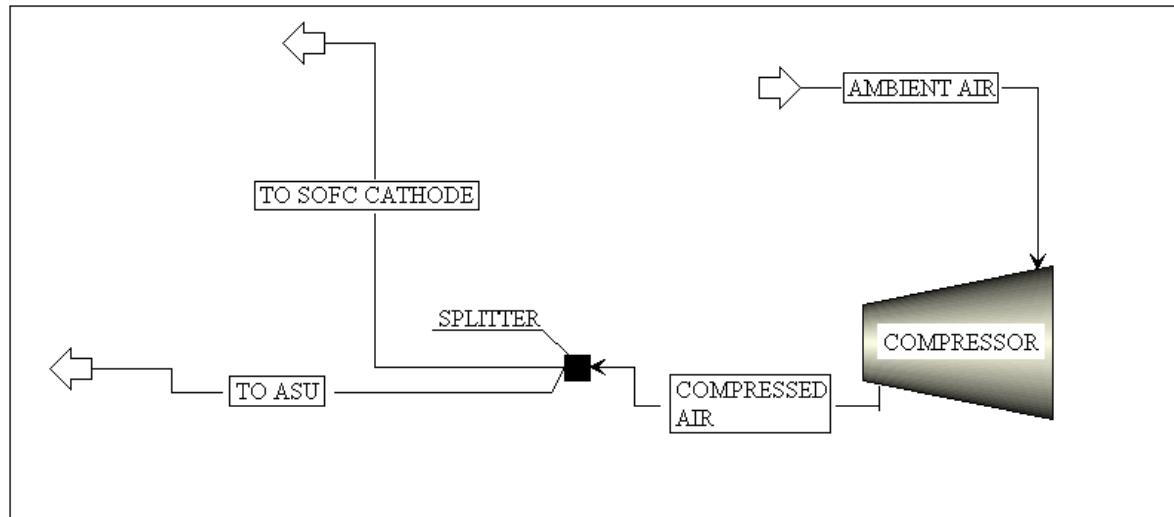


Figure 20: Air compression for the fuel cell and for the ASU (Aspen Plus)

The configuration of this system is shown in Fig. 20. The specifications of the compressor are shown in figure 21. The compressor works as isentropic and the discharge pressure is set to be 15,1 bars, with the isentropic efficiency of 88% and the mechanical efficiency of 0,98.

Specifications	Calculation Options	Power Loss	Convergence	Integration Parameters	Utility
<b>Model and type</b>					
Model: <input checked="" type="radio"/> Compressor <input type="radio"/> Turbine					
Type: <input type="text" value="Isentropic"/>					
<b>Outlet specification</b>					
<input checked="" type="radio"/> Discharge pressure: <input type="text" value="15,1"/> <input type="text" value="bar"/>					
<input type="radio"/> Pressure increase: <input type="text"/> <input type="text" value="bar"/>					
<input type="radio"/> Pressure ratio: <input type="text"/>					
<input type="radio"/> Power required: <input type="text"/> <input type="text" value="kW"/>					
<input type="radio"/> Use performance curves to determine discharge conditions					
<b>Efficiencies</b>					
Isentropic: <input type="text" value="0,88"/> Polytopic: <input type="text"/> Mechanical: <input type="text" value="0,98"/>					

Figure 21: Specifications of the compressor model (Aspen Plus)

## 2.4 Modeling of CO<sub>2</sub> preparation for sequestration

After the tail-gas processing a CO<sub>2</sub> rich stream, at relatively low pressures, is created consisting mainly of CO<sub>2</sub> and water (with some N<sub>2</sub> and H<sub>2</sub>, traces of CO and CH<sub>4</sub>). This stream has to be compressed up to 150 bars and the water has to be knocked out of the stream. The water knock-out takes place via a refrigeration plant, and to model this, a simple heat exchanger is used which cools the CO<sub>2</sub>-rich stream down to -30°C. In addition the

cooling keeps the temperature at the outlet of the compressor reasonable. To find out how much power is needed for the refrigeration plant to work the following equation was used:

$$\beta = \frac{Q_{in}}{W_{cycle}} \rightarrow W_{cycle} = \frac{Q_{in}}{\beta} \quad [2.2]$$

Where  $\beta$ -coefficient of performance, it was chosen to be 2;  $Q_{in}$  – amount of energy received by the system, heat duty [Gcal/hr];  $W_{cycle}$  – net work into the system to accomplish this effect. The power input to the refrigeration plant was calculated in an Excel spreadsheet where the input is the heat duty of the heat exchanger and the output is the electrical power input to that plant. This value was used later to calculate the net-power of the system. The specifications of the compressor are the same as the air compressor, except the discharge pressure is 150 bars.

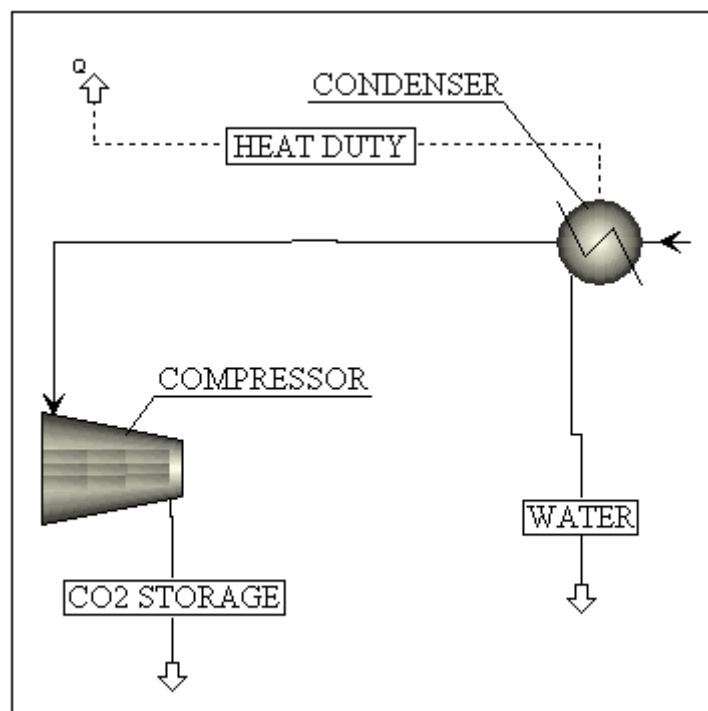


Figure 22: Preparation of CO<sub>2</sub> for storage (Aspen Plus)

## 2.5 Gas turbine modeling

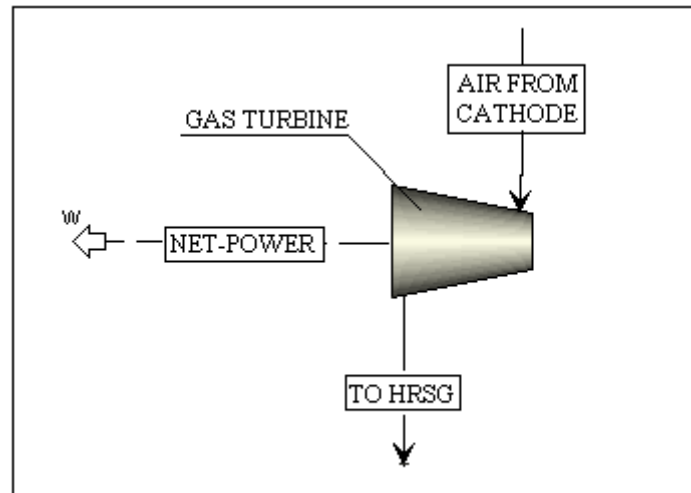


Figure 23: Gas turbine model (Aspen Plus)

The SOFC uses a combined Brayton-Rankine cycle as a bottoming cycle. For the Brayton cycle, gas turbine cycle, the type of the turbine is isentropic, the isentropic efficiency is 90%, the mechanical efficiency, like the compressors, is 98% and the discharge pressure was said to be 1,01 atm. The modeling of the gas turbine is fairly simple, an expander was used. After gases are expanded they are sent to the heat recovery steam generator, and the produced steam will be utilized in a steam turbine.

The screenshot shows the 'Specifications' tab of the Aspen Plus interface for a gas turbine model. The 'Model and type' section has 'Model' set to 'Turbine' and 'Type' set to 'Isentropic'. The 'Outlet specification' section has 'Discharge pressure' set to '1,01 atm'. The 'Efficiencies' section has 'Isentropic' set to '0,9' and 'Mechanical' set to '0,98'.

Figure 24: Gas turbine model specifications (Aspen Plus)

Only air will go to the gas turbine. After the SOFC the temperature of the air is around 800°C. The additional heat comes from burning the fuel left in the depleted syngas, directly in the air stream or transferring the heat to the air stream via a heat exchanger. Net-power at the power output of the expander is due to the fact that a user defined model sums up all the power generated and consumed in the system and overwrites that number with the net-power produced. This is explained further on in this chapter.

## 2.6 Steam cycle (Rankine cycle) modeling

The role of the steam turbine will be taken into account in a simplified way. Heat exchangers are placed at the exhaust of the gas turbine (Fig. 25), before the knock-out of water from the

CO<sub>2</sub>-rich stream takes place and at some other places (compressor with intercooling) depending on the system configuration. The power output of the Rankine cycle is calculated using the heat duties of these heat exchangers.

$$\dot{W}_{Rankine\ BC} = \eta_{Rankine} \times \sum \dot{Q}_{in} = \eta_{Rankine} \times [\dot{E}_{GT\ rej} + \dot{Q}_{CO_2} + \dots]$$

Where  $\eta_{Rankine}$  is the efficiency of the Rankine cycle and is set here 0,3;  $\sum \dot{Q}_{in}$  is the sum of heat sources in the system which could be used for steam generation and the temperature of the cycle exhaust will be 126°C [1.12].

For converting Gcal/hr into kW the following relationship was used:

$$1\text{ Gcal/hr} = 1163,09\text{ kW}$$

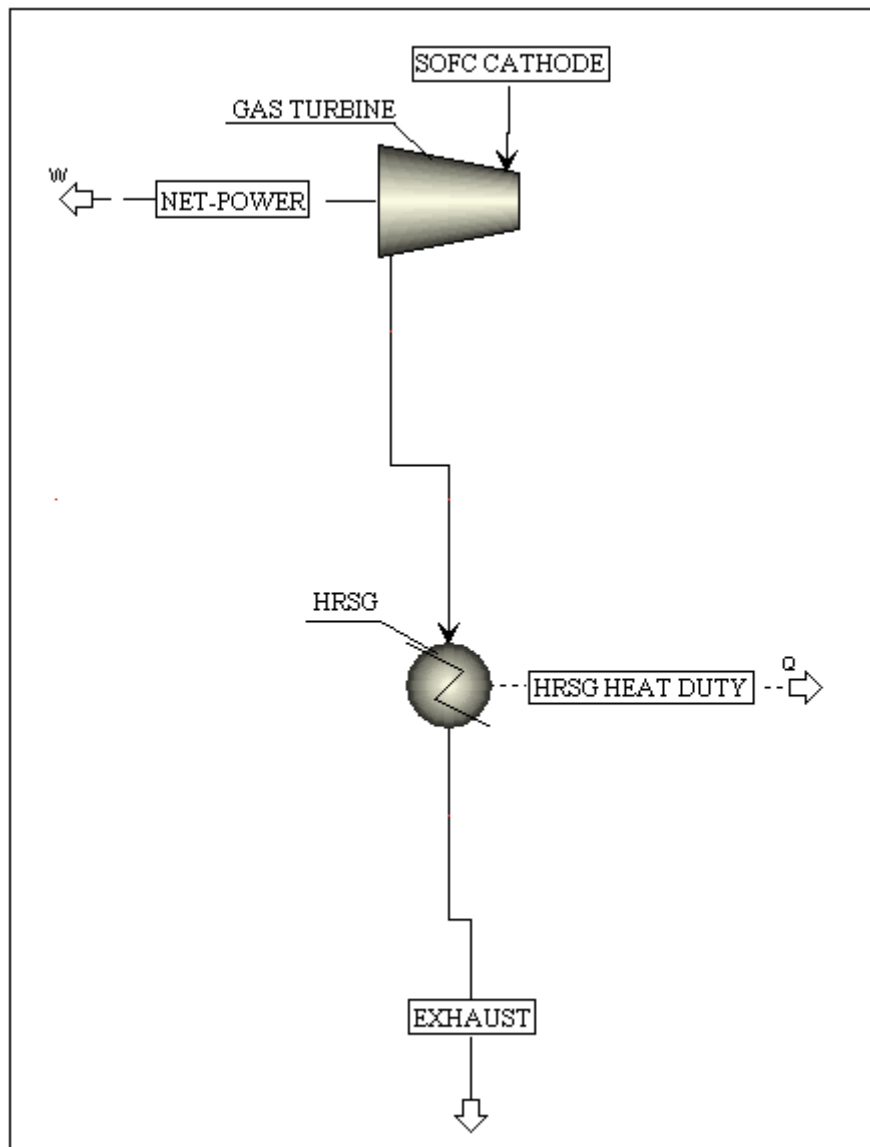


Figure 25: HRSG model (Aspen Plus)

## 2.7 Modeling of H<sub>2</sub>-conducting membrane

It has been found that H<sub>2</sub> permeates through the membrane via a solution-diffusion mechanism, and the rate of H<sub>2</sub> permeation per unit area of the membrane,  $J_{H_2}$  (mol/(m<sup>2</sup>s)), is proportional to the partial pressure difference. The calculations for the membrane were done using an Excel spreadsheet. Inputs to the membrane model are taken from Aspen Plus, which are the contents and parameters of the retentate and permeate streams; the membrane model then conducts the calculations and exports the results to Aspen.

The H<sub>2</sub> flux through the membrane is calculated as follows:

$$J_{H_2} = A \times k \times (P_{H_2,ret}^n + P_{H_2,perm}^n) \quad [2.3]$$

Where A is the surface area of the membrane [m<sup>2</sup>]; k is the apparent permeability of the membrane material [mol/(m<sup>2</sup>Pa<sup>0.5</sup>)];  $P_{H_2,ret}^n$  is the partial pressure of H<sub>2</sub> on the retentate side [Pa];  $P_{H_2,perm}^n$  is the partial pressure of H<sub>2</sub> on the permeate side [Pa].

This formula applies when the limiting process of the H<sub>2</sub> permeation through the membrane is the bulk diffusion in the membrane material. The bulk diffusion is the limiting process only if the membrane is thick enough. If the membrane is very thin, some other processes of the permeation will be the limiting ones.

Because we have a solid metal membrane and only hydrogen atoms diffuse through the membrane the exponent n is 0,5. In contrast if there would be a microporous membrane where only hydrogen molecules pass through the membrane the exponent n would be 1.

The flux of H<sub>2</sub> through the membrane depends on the partial pressure difference of the H<sub>2</sub> on either side of the membrane. The partial pressure depends on the total pressure on each side of the membrane and also on the molar fraction of H<sub>2</sub> in the gas. These parameters can be controlled. Permeation of H<sub>2</sub> to the permeate side is favored if the pressure on the retentate side is big and is low on the permeate side. In addition a sweep gas can be used on the permeate side. This has two effects: first, it carries away the H<sub>2</sub>, and second, it dilutes the H<sub>2</sub>, lowering the partial pressure of the H<sub>2</sub> in the stream. This also has a negative effect: the H<sub>2</sub> stream is diluted and lower temperatures will be achieved in the combustor later on.

Several different gases can be used as sweep gas, for example: air, nitrogen, argon and even with no sweep gas. In this study air and nitrogen were used.

The membrane was divided into 30 stages to simulate the partial pressure changes of H<sub>2</sub> along the length of the membrane and thus the changes in the permeation flux. A co-current flow was chosen. For every step the flux, molar flow of H<sub>2</sub>, total molar flow, mole fraction and partial pressure of H<sub>2</sub>, and the total pressure were recalculated for both the retentate and permeate side:

Retentate side

$$\text{Molar flow of H}_2: \dot{v}_i^{H_2} = \dot{v}_{i-1}^{H_2} - J_{i-1}^{H_2} \quad [mol/s]$$

$$\text{Total molar flow: } \dot{v}_i^{total} = \dot{v}_{i-1}^{total} - J_{i-1}^{H_2} \quad [mol/s]$$

$$\text{Mole fraction of H}_2: x_i^{H_2} = \dot{v}_i^{H_2} / \dot{v}_i^{total} \quad [-]; \dot{v}_i^{total} = \sum_j \dot{v}_n^j \quad [mol/s]$$

$$\text{Partial pressure of H}_2: P_j = x_j \times P_i^{total} \quad [Pa]$$

$$\text{Total pressure: } P_i^{total} = P_{i-1}^{total} - (P_{i-2}^{H_2,ret} - P_{i-1}^{H_2,ret}) \quad [mol/s]$$



Permeate side

Molar flow of H<sub>2</sub>:  $\dot{v}_i^{H_2} = \dot{v}_{i-1}^{H_2} + J_{i-1}^{H_2} [\text{mol/s}]$

Total molar flow:  $\dot{v}_i^{total} = \dot{v}_{i-1}^{total} + J_{i-1}^{H_2} [\text{mol/s}]$

Total pressure:  $P_i^{total} = P_{i-1}^{total} + (P_{i-1}^{H_2,ret} - P_{i-2}^{H_2,ret}) [\text{mol/s}]$

Due to the fact that there is a partial pressure difference needed for the permeation process to take place, the recovery of 100% of the H<sub>2</sub> from the retentate stream is not likely to happen (unless a constant vacuum is created on the permeate side and the surface area of the membrane is very large).

The imported values from Aspen are the temperature, pressure and the molar flows of species of the retentate and sweep gas (if there is one) streams on the inlet. The exports to Aspen are the same values but on the outlet of the membrane.

It is assumed that a pressure change takes place on both sides of the membrane; this is based on the fact that a mass transfer takes place in the form of H<sub>2</sub> permeating through the membrane but the volume stays same. The pressure on the retentate side decreases as much as the partial pressure of H<sub>2</sub> changes across the retentate side of the membrane, and the pressure on the permeate side increases as much as the partial pressure of H<sub>2</sub> changes across the permeate side of the membrane.

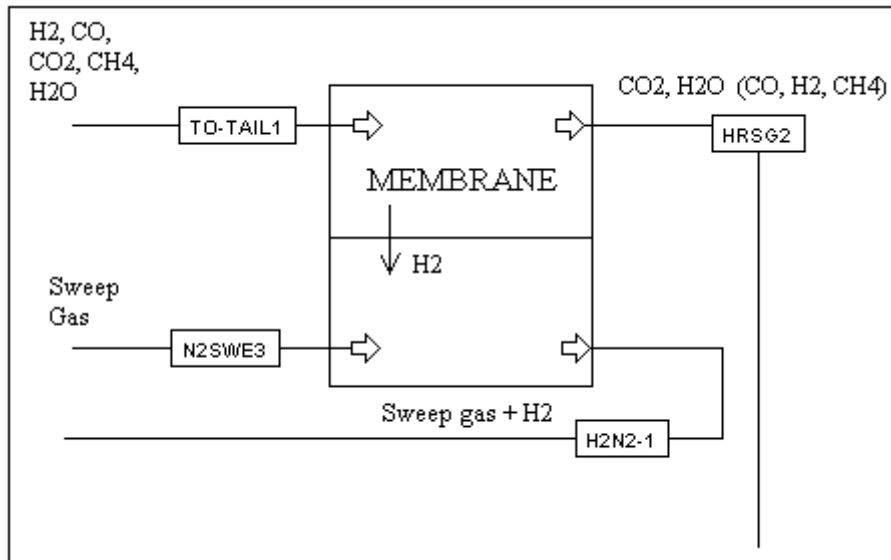


Figure 26: H<sub>2</sub> conducting membrane

As seen on Fig. 26, the membrane results in a CO<sub>2</sub> and H<sub>2</sub>O-rich stream and a mixture of sweep gas (if used) H<sub>2</sub>. The H<sub>2</sub>-rich gas stream can later be fed into a combustor. The combustion product of H<sub>2</sub> is water, and this way emissions are eliminated and water from the CO<sub>2</sub> stream can be relatively easily knocked out via cooling.

## 2.8 Modeling of O<sub>2</sub>-conducting membrane

The approach to simulating the O<sub>2</sub> conducting membrane is finding out how much fuel (CH<sub>4</sub>, CO and H<sub>2</sub>) is left in the tail-gas and withdrawing as much O<sub>2</sub> from the depleted air stream, from the cathode of the SOFC, as needed to oxidize all of it. The amount of O<sub>2</sub> is calculated as follows:

$$\dot{v}_{OXYGEN} = 2 \times \dot{v}_{SYNGAS2}^{CH_4} + (\dot{v}_{SYNGAS2}^{CO} + \dot{v}_{SYNGAS2}^{H_2})/2 \text{ [kmol/hr]}$$

The actual membrane operation was not calculated, because the changes in mass flows are of interest. The concept is similar to the oxy-combustor; the only difference is that the O<sub>2</sub> is taken from the depleted air stream, which comes from the SOFC cathode.

The inputs to the O<sub>2</sub> membrane model are the molar flows of fuel species in the tail-gas stream and the species of depleted air from the SOFC cathode. In addition the temperature and pressure of these streams are read to import them to the streams exiting the membrane.

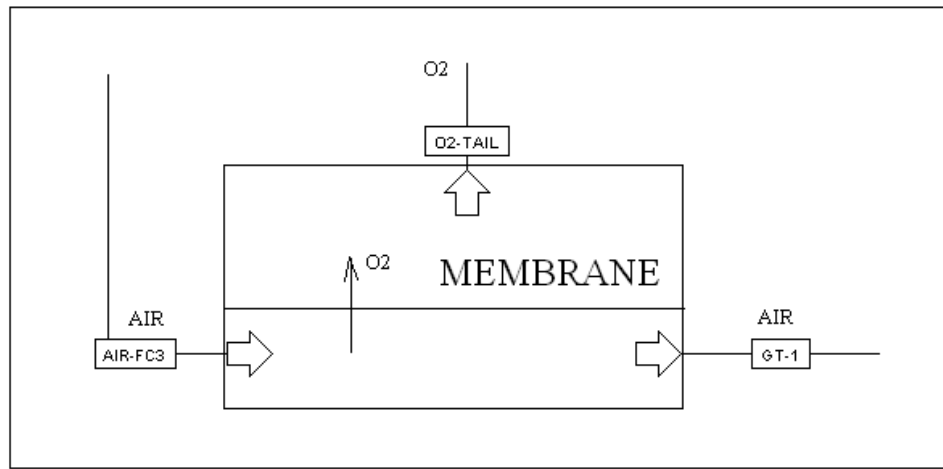


Figure 27: O<sub>2</sub> conducting membrane (Aspen Plus)

## 2.9 Parasitic losses from ASU

The power needed for the air separation unit (ASU) was taken into account. From the literature the power needed to separate 1 kg of O<sub>2</sub> from air in 1 second was 0,424 MW/(kgs). It is assumed that this includes also the power for compression. To get the power consumption in the ASU, the power needed to compress 1 kg of O<sub>2</sub> per second was calculated:

$$P_{compress}^{O_2} = P_{compress}^{air} / m_{air} \times x_{O_2} \text{ [MW/(kgs)]}$$

Where  $P_{compress}^{O_2}$  is the power needed to compress 1 kg of [Mw/(kg/s)];  $P_{compress}^{air}$  is the power needed to compress all the air (to ASU and SOFC cathode) [MW];  $m_{air}$  is the total mass flow of air entering the compressor [kg/s];  $x_{O_2}$  is the weight fraction of O<sub>2</sub> in the air.

The previously calculated value is subtracted from the value mentioned in the beginning of this chapter:

$$P_{ASU}^{O_2} = P_{ASU+Compr}^{O_2} - P_{compress}^{O_2} \text{ [MW/(kgs)]}$$

Where  $P_{ASU}^{O_2}$  is the power needed in the ASU [MW/(kgs)];  $P_{ASU+Compr}^{O_2}$  is the power needed in the ASU and compressor to get 1 kg of  $O_2$  [MW/(kgs)];  $P_{compress}^{O_2}$  is the power to compress 1 kg of  $O_2$ .

The previous calculations are made in order to get values which do not depend on the flows. This becomes handy when, for example, an oxy-combustor is integrated into the system, and then extra  $O_2$  needs to be produced in the ASU and extra air needs to be compressed to be sent to the ASU. By knowing the needed amount of extra  $O_2$  the parasitic losses can easily be calculated.

## 2.10 Modeling of oxy-combustion

To model oxy-combustion a Gibbs reactor was used, which is based on rigorous reaction and/or multiphase equilibrium based on Gibbs free energy minimization. In order to supply the amount of pure oxygen to the reactor for oxidizing all the fuel left in the depleted anode stream an Excel spreadsheet was used. Inputs to the Excel spreadsheet are the molar flows of  $H_2$ ,  $CO$  and  $CH_4$  in the anode stream. The flows of species and the total oxygen flow to the reactor are calculated as follows:

$$\dot{v}_{oxygen}^{O_2} = 2 \times \dot{v}_{anode}^{CH_4} + (\dot{v}_{anode}^{H_2} + \dot{v}_{anode}^{CO})/2 \text{ [kmol/hr]}$$

$$\dot{v}_{oxygen}^{N_2} = 0,95 \times \dot{v}_{oxygen}^{O_2} \text{ [kmol/hr]}$$

$$\dot{v}_{oxygen} = \dot{v}_{oxygen}^{N_2} + \dot{v}_{oxygen}^{O_2} \text{ [kmol/hr]}$$

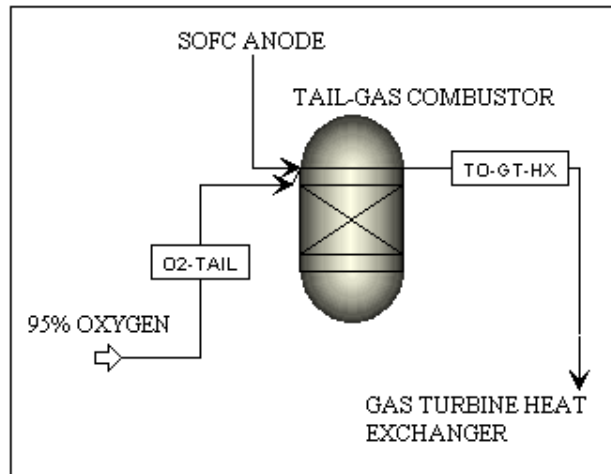


Figure 28: Oxy-combustor

The combustion products will not be fed directly to the gas turbine; instead a heat exchanger is used to raise the temperature of the depleted air from the SOFC cathode.

## 2.11 Modeling of H<sub>2</sub>-conducting membrane reactor with N<sub>2</sub> as sweep gas

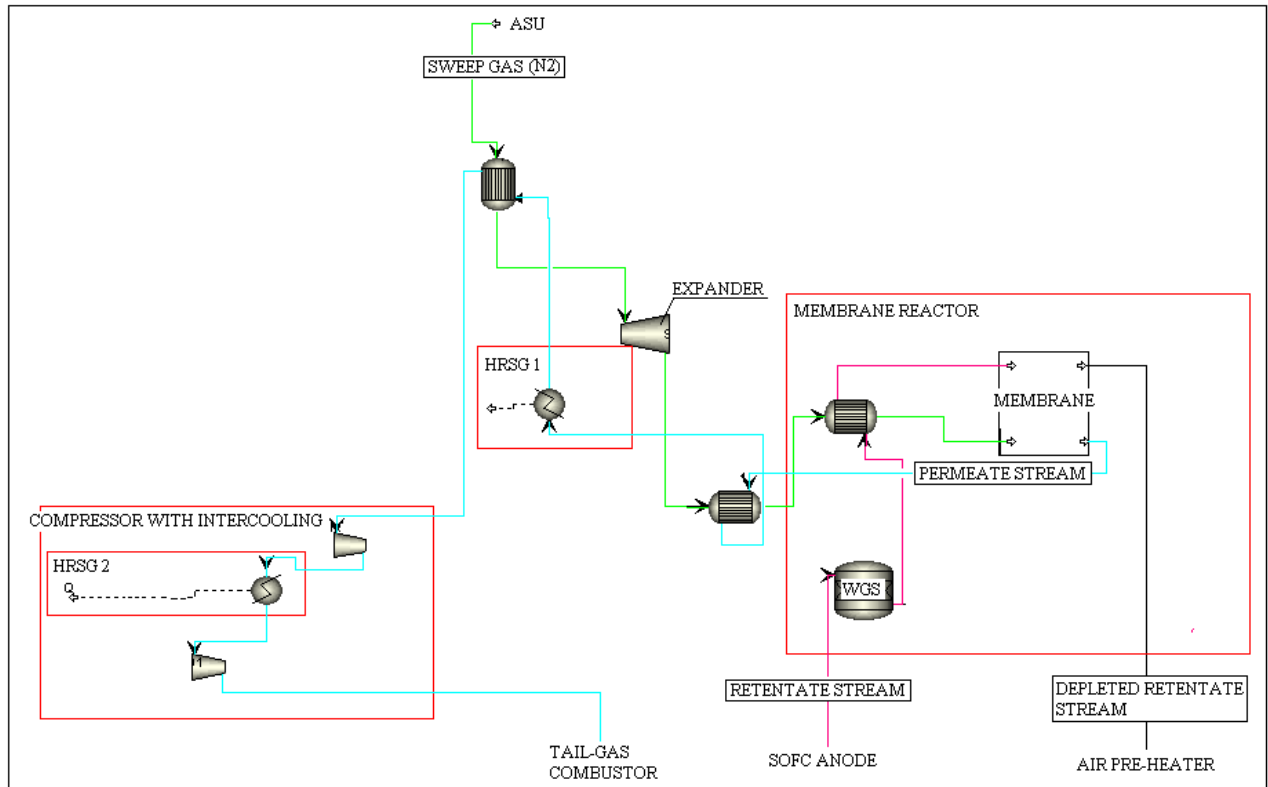


Figure 29: Concept of H<sub>2</sub>-conducting membrane reactor with N<sub>2</sub> as sweep gas

In Fig. 29 the concept of an H<sub>2</sub>-conducting membrane with N<sub>2</sub> as sweep gas is presented.

The following processes take place in the membrane reactor:

- Water-Gas Shift Reaction
- Transfer of H<sub>2</sub> from the retentate side to the permeate side
- Heat transfer

It was assumed that all the CO and CH<sub>4</sub> in the depleted syngas shifts on the inlet of the membrane, allowing the use of a stoichiometric reactor where the fraction of reactants reacted can be determined.

The inputs to the membrane reactor were adjusted in such a way that the recovery of the H<sub>2</sub> from the retentate stream is 90%.

In addition the membrane works as a heat exchanger, because the membrane itself is very thin (much less than 1 mm). To model the heat exchanger function in front of the membrane model the retentate and sweep gas streams flow through a heat exchanger and the difference between the outlet was set 20°C.

N<sub>2</sub> from the ASU was used as the sweep gas. The sweep gas from the ASU is at relatively high pressure (3,6 bar) and to avoid high partial pressure of H<sub>2</sub> on the permeate side, which has a negative effect on the permeability, the total pressure must be lowered, thus an expander was used.

Using an expander requires heating the gas before and after the expander due to the fact that the temperatures may drop too low ( $N_2$  from ASU is at  $7^\circ\text{C}$ ) and dangerous thermal gradients may occur in the membrane. After the membrane the mixture of  $H_2$  and sweep gas, the permeate stream, has a low pressure (0,1-0,2 bar) but the tail gas combustor operates at 14,7 bars. The permeate stream must be compressed at least to the pressure at which the combustor is operating. A compressor with intercooling was used because of the temperature constraints of the compressor, here set to be  $450^\circ\text{C}$ . The heat from the intercooling is used to produce steam for the Rankine cycle.

## 2.12 Modeling of $H_2$ -conducting membrane reactor with air as sweep gas

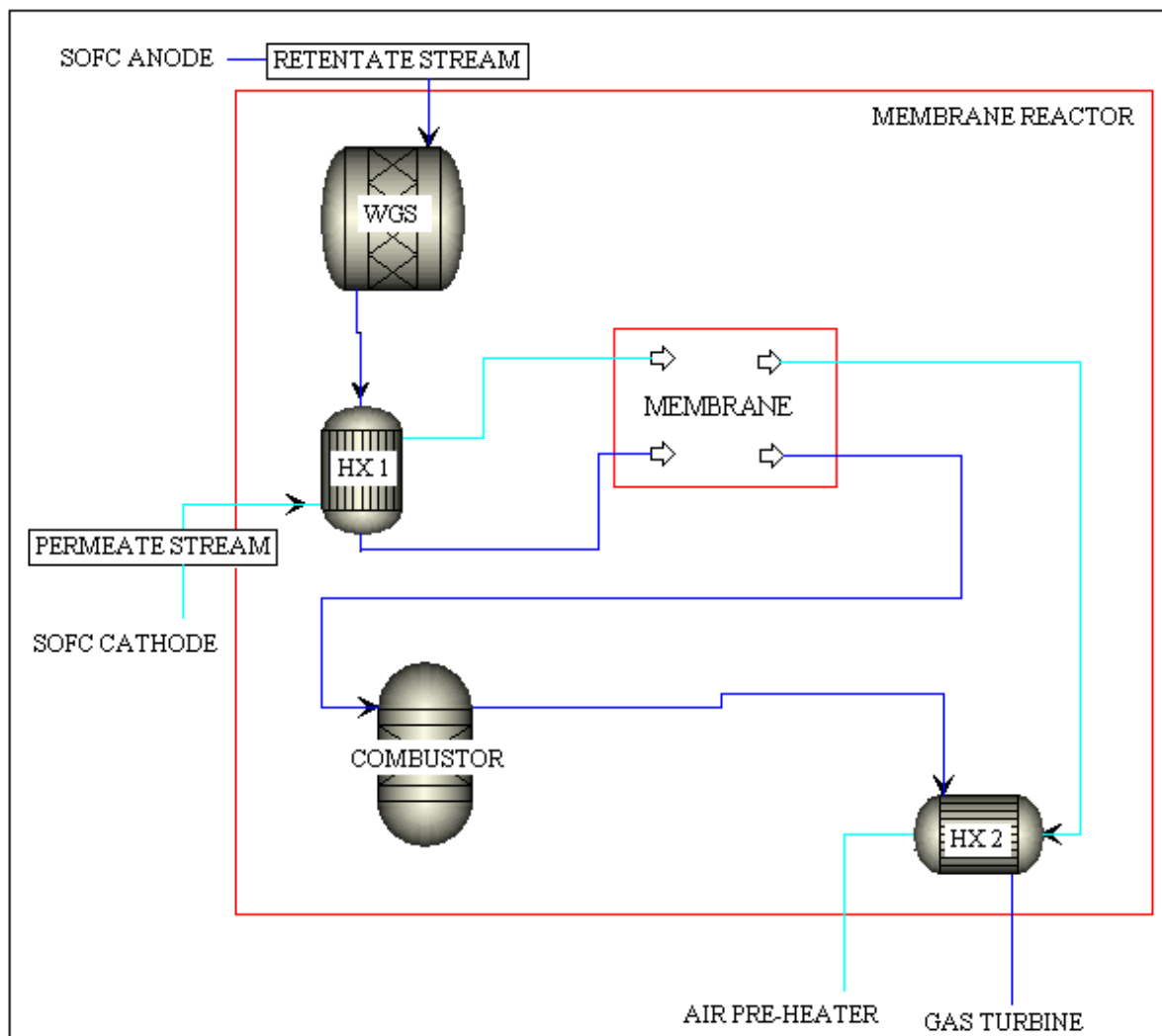


Figure 30: Concept of  $H_2$ -conducting membrane reactor with air as sweep gas

The model for the  $H_2$ -conducting membrane with air as sweep gas is presented on Fig. 30. Several processes happen at the same time:

- Water-Gas Shift Reaction
- Transfer of  $H_2$  from the retentate side to the permeate side

- Oxidation of  $H_2$
- Heat transfer

It is assumed that all the CO and  $CH_4$  are shifted in the entrance of the membrane reactor. To simulate this, a stoichiometric reactor was placed before the membrane model. The fractional conversion of both CO and  $CH_4$  is 1.

In the membrane model around 90% of the  $H_2$  in the retentate stream is transferred to the air side of the membrane. The membrane model is described in chapter 2.7.

After this the mixture of air and  $H_2$  is fed to another reactor (Gibbs free energy reactor) where the combustion of  $H_2$  takes place and the temperature of air rises.

The membrane reactor also acts as a heat exchanger, and to model this, two heat exchangers are used (Fig. 30): one is between the water gas shift reactor and the membrane and the second one is after the combustor. The heat exchangers are needed because otherwise the heat transfer to the retentate side is not taken into account and the temperature of the air on the outlet of the MR is higher than it should be.

These simplified approaches are justified because the temperature and pressure affects only how much surface area of the membrane is needed to permeate a certain amount of  $H_2$ , and the aim is to look at the problem from a system point of view to compare flows and power output of different concepts.

The advantage of this concept, compared to using  $N_2$  as sweep gas, is that the system is less complex. All the processes take place in one unit and the following components do not have to be used:

- compressors
- expanders
- heat exchangers
- external source of sweep gas

On the negative side it can be mentioned that the temperature during oxidizing the  $H_2$  in air may raise the temperatures higher than the membrane material is able to withstand.

## 2.13 Modeling of O<sub>2</sub>-conducting membrane reactor

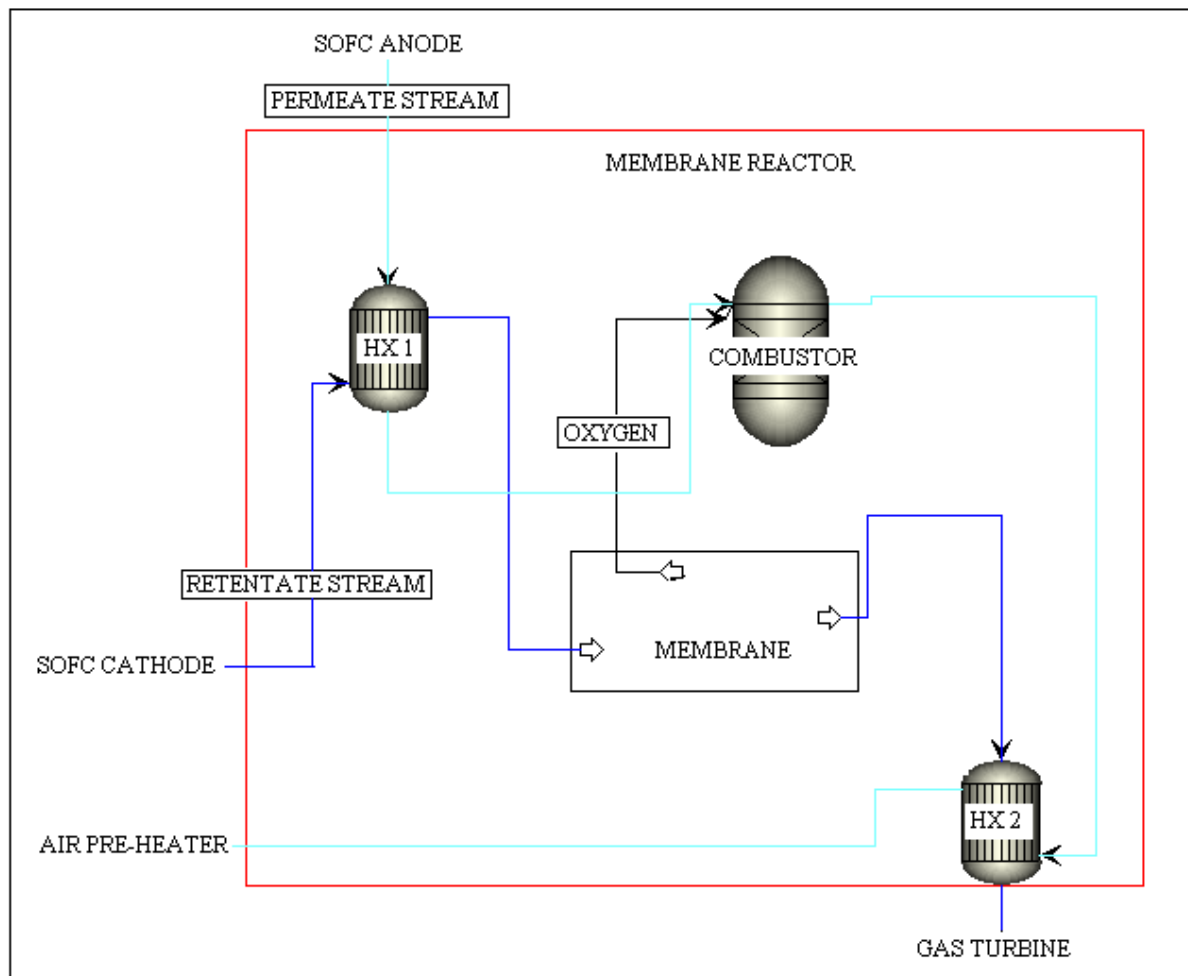


Figure 31: Concept of O<sub>2</sub>-conducting membrane reactor

The concept of an O<sub>2</sub>-conducting membrane reactor is presented in Fig. 31. The following takes place in the membrane reactor:

- Transfer of O<sub>2</sub> from the air side to the depleted fuel side
- Heat transfer
- Oxidation of CO, CH<sub>4</sub> and H<sub>2</sub>

In the O<sub>2</sub>-conducting membrane, O<sub>2</sub> from the air is permeating through the membrane without mixing the two streams from the cathode and anode, and by oxidizing the CO, CH<sub>4</sub> and H<sub>2</sub> in the depleted syngas a high purity CO<sub>2</sub> stream is created.

The oxidation takes place in a Gibbs free energy reactor. The membrane reactor model also has two heat exchangers in it because the thickness of the membrane separating the two gas streams is very thin and, thus, heat transfer takes place.

The advantage of this concept compared to oxy-combustion is that no additional energy is spent on compressing additional air for the ASU and separating O<sub>2</sub> in the ASU. On the other hand, oxy-combustion is a fairly simple and developed technology while oxygen conducting membranes are in the phase of development, and some R&D has to be done in order for this to be commercially feasible.

Currently the flux of O<sub>2</sub> through the oxygen conducting membranes is relatively low and the stability in the aggressive environment of syngas at elevated temperatures and pressures is questionable. If these can be solved the O<sub>2</sub> conducting membranes would improve the efficiency of the plants. In addition the O<sub>2</sub> conducting membrane may replace the ASU.

## 2.14 Net power output calculations

For the net power calculations the power is generated in the:

- SOFC
- Gas Turbine
- Rankine Cycle
- Expansion of sweep gas

And consumed in the:

- Air Compressor
- Refrigeration plant for water knock-out from CO<sub>2</sub> rich stream
- Compression of CO<sub>2</sub> for storage
- Compression of permeate stream
- ASU

Those which are taken into account for a certain concept depends on the system configuration (Table 14).

After the net-power calculations have been done the efficiencies are calculated. This is done by dividing the net-power with power (based on the LHV and HHV) from the coal slurry fed to the gasifier. In addition, the efficiencies without the power needed for water knock-out and compressing the CO<sub>2</sub> for storage are calculated in order to compare the power production of each concept and to compare the drop in efficiency caused by the CO<sub>2</sub> preparation for storage.

## 2.15 Inputs to the model

There are two inputs to this model: the syngas and the air flow to the compressor. The content and flows of the syngas and air are presented in table 9. The syngas and air content, and other parameters, were taken from the Fuel Cell Handbook [1.12], p 67. The mass flow of syngas to the fuel cell that was taken was half of what was in the Fuel Cell Handbook. The air flow was chosen to be 9 times the flow of syngas.

Description	T	P	Mass Flow	Mole Flow	CH <sub>4</sub>	CO	CO <sub>2</sub>	H <sub>2</sub>	H <sub>2</sub> O	H <sub>2</sub> S	N <sub>2</sub> +Ar	NH <sub>3</sub>	O <sub>2</sub>
	°C	bar	t/h	kmol/hr	%	%	%	%	%	%	%	%	%
Clean Syngas	399	15	56,5	2950	0,3	42,3	9,5	35,8	9,6	trace	1,5	0,2	
Air	20	0,98	TBS*	TBS*			trace		1,1		78,1		20,8

\*TBS – to be specified

Table 9: Content and other parameters of syngas and air fed to the system



## 2.16 Chapter References

- 2.1 R.J. Braun, "Modeling, Analysis, and Optimization of IGFC Systems (Task I-C), presentation prepared for the U.S. Department of Energy, National Energy Technology Laboratory, Pittsburgh, PA October (2008)
- 2.2 Moran, Shapiro, *Fundamentals of Engineering Thermodynamics 6<sup>th</sup> Edition*, Wiley 2007 p 67
- 2.3 Iyoha, *H<sub>2</sub> Production in Palladium & Palladium-Copper Membrane Reactors at 1173K in The Presence of H<sub>2</sub>O*, Ph.D. Thesis, University of Pittsburgh – 2007
- 2.4 [http://en.wikipedia.org/wiki/First\\_law\\_of\\_thermodynamics](http://en.wikipedia.org/wiki/First_law_of_thermodynamics) - web page

### 3 Results

In Fig. 32 the flow sheet of the IGFC is presented. In the empty square the different tail-gas concepts can be applied. Only the simple tail-gas combustor where the anode and cathode streams are mixed is different and is presented on Fig 33.

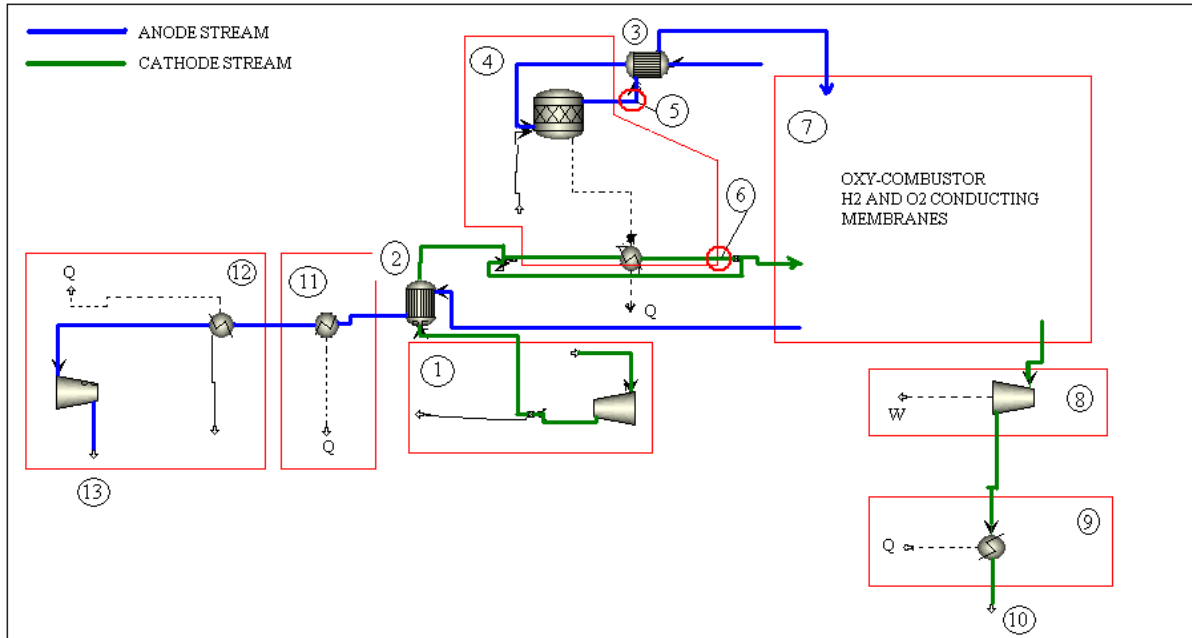


Figure 32: Flow sheet of IGFC (CO<sub>2</sub> capture)

1. Air compressor
2. Air pre-heater
3. Syngas pre-heater
4. SOFC
5. SOFC anode
6. SOFC cathode
7. Tail-gas concept
8. Gas turbine
9. HRAG 1
10. Exhaust (air)
11. HRSG 2
12. Water knock-out and compression of CO<sub>2</sub>
13. CO<sub>2</sub> storage

If the CO<sub>2</sub> is vented some of the components (water knock-out and compression of CO<sub>2</sub>), compared to if CO<sub>2</sub> is captured, are not needed.

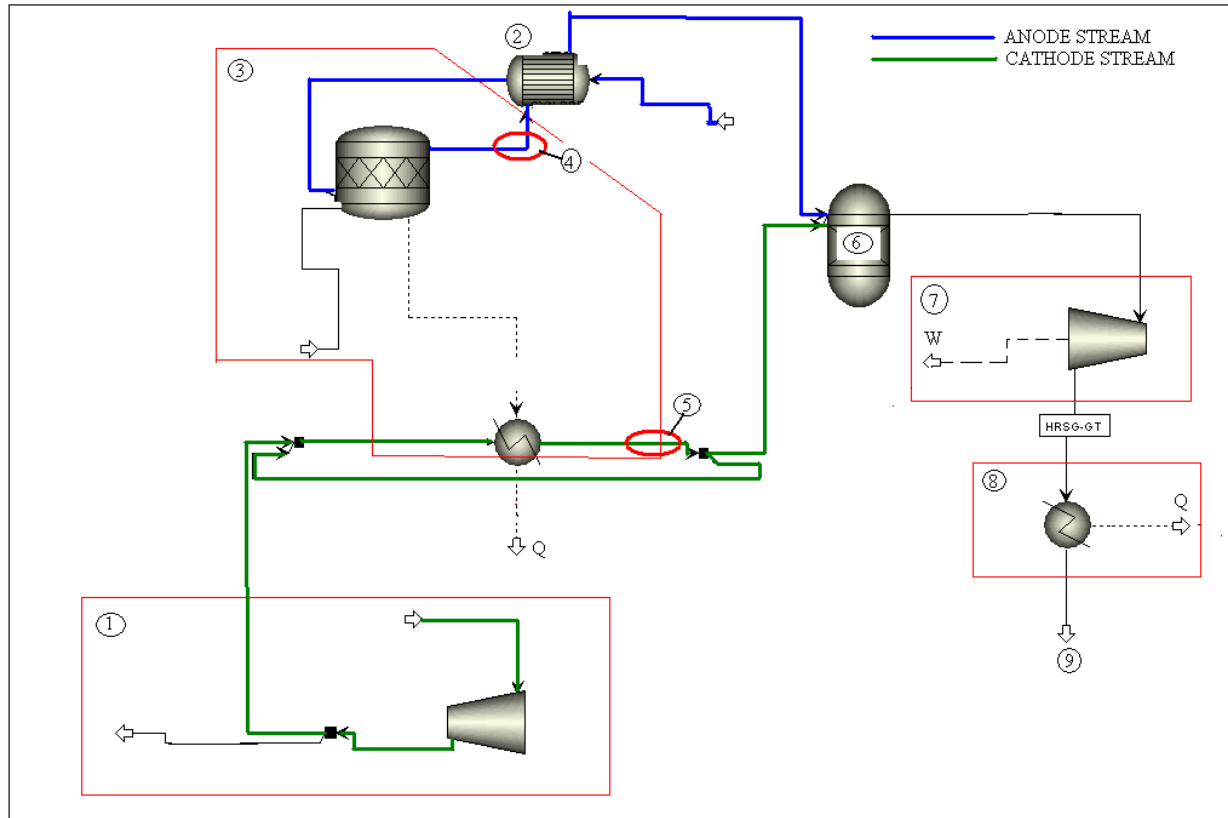


Figure 33: Flow sheet of IGFC (venting of CO<sub>2</sub>)

1. Air compressor
2. Syngas pre-heater
3. SOFC
4. SOFC anode
5. SOFC cathode
6. Tail-gas combustor
7. Gas turbine
8. HRSG
9. Exhaust (Air)

The following results are presented:

1. Air compressed and split fractions going to the ASU and the SOFC cathode
2. Fraction and flows of depleted air needed to be recycled in order to have 650°C in the SOFC cathode inlet
3. H<sub>2</sub> recovered and/or combusted in the anode stream
4. Temperature and properties of air going to the gas turbine
5. The content and properties of the CO<sub>2</sub>-rich stream sent to storage
6. Net power of the system and the breakdown of where and how much power is produced/consumed
7. Overall efficiencies of the system with capture and without capture
8. Drop in efficiency caused by the preparation of CO<sub>2</sub> for storage

	Tail-gas combustor	Oxy-combustion	H <sub>2</sub> -MR, N <sub>2</sub> -sweep	H <sub>2</sub> -MR, air sweep	O <sub>2</sub> -MR
--	--------------------	----------------	---	-------------------------------	--------------------

<b>Split fraction recycled</b>	<b>0,63</b>	<b>0,53</b>	<b>0,60</b>	<b>0,53</b>	<b>0,53</b>
<b>kg air recycled per kg air inlet</b>	<b>1,62</b>	<b>1,08</b>	<b>1,43</b>	<b>1,09</b>	<b>1,09</b>
<b>Temp. before recycling [°C]</b>	<b>399</b>	<b>483</b>	<b>428</b>	<b>482</b>	<b>482</b>

*Table 10: Split fraction of cathode air recycled*

In all cases the air enters the compressor at ambient temperature (20°C) and pressure (0,98 bar), and is compressed to 15,1 bars. The temperature rises to 399°C. In every concept, except the tail-gas combustor, the air is pre-heated with the heat from the CO<sub>2</sub> rich stream, but this heat is not sufficient to increase the temperature of air up to 650°C. To overcome this by not using external heat sources, the recycled cathode stream is used.

As shown in table 10, the lower the temperature of the air before the cathode, the more cathode outlet air per kilogram of air fed to the cathode has to be recycled. It can also be seen that the higher the air temperature is before the recycling the more air has to be compressed for the cathode.

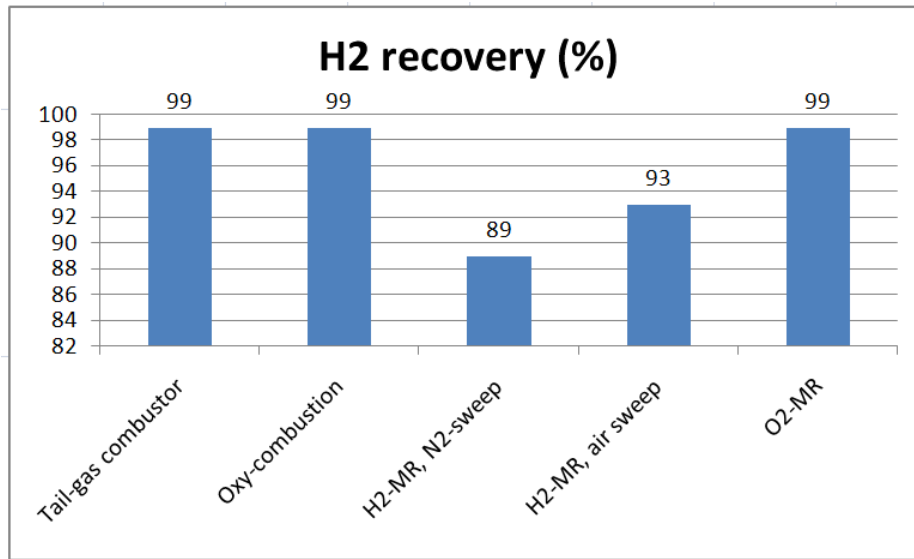


*Figure 34: H<sub>2</sub> recovery [%]*

In figure 34 the H<sub>2</sub> recovery is presented. The recovery percentage shows how much H<sub>2</sub> is reacted in a useful way, the H<sub>2</sub> that was not recovered was stored together with the CO<sub>2</sub>; this is in the case of H<sub>2</sub>-conducting membranes due to the nature of H<sub>2</sub>-membranes, where the recovery of 100% of H<sub>2</sub> is not easily achievable.

Regarding the higher H<sub>2</sub> recovery for the H<sub>2</sub>-conducting membrane with air as sweep gas (figure 34), the reason for this is the fact that there is air on the permeate side and H<sub>2</sub> reacts with O<sub>2</sub> right after permeation. It was assumed that the partial pressure of H<sub>2</sub> on the permeate side remains close to zero along the whole membrane and thus higher permeation rates occur, compared to when N<sub>2</sub> is used as sweep gas.

	<b>Tail-gas combustor</b>	<b>Oxy-combustion</b>	<b>H<sub>2</sub>-MR, N<sub>2</sub>-sweep</b>	<b>H<sub>2</sub>-MR, air sweep</b>	<b>O<sub>2</sub>-MR</b>
<b>Temperature inlet [°C]</b>	937	920	954	897	922
<b>Temperature outlet [°C]</b>	425	388	411	374	385
<b>Mass flow to GT [kg/hr]</b>	538000	579900	514400	589700	575700
<b>Power generated [kW]</b>	90400	95600	88300	96600	94900
<b>Power for compressing air</b>	62900	80900	68500	78200	77600
<b>Net power from GT</b>	27500	14700	19700	18300	17400

*Table 11: Properties of the gas turbine*

On table 11 the properties of the media flowing through the gas turbine are presented and in addition the power generated and consumed by the gas turbine is presented. The power generated and consumed is directly related to the amount of air flowing through the gas turbine. Temperature has less effect.

	<b>Tail-gas combustor*</b>	<b>Oxy-combustion</b>	<b>H<sub>2</sub>-MR, N<sub>2</sub>-sweep</b>	<b>H<sub>2</sub>-MR, air sweep</b>	<b>O<sub>2</sub>-MR</b>
<b>Temperature [°C]</b>	126	126	174	188	91
<b>Pressure [bar]</b>	1,023	150	150	150	150
<b>Mass flow [kg/hr]</b>	538000	69300	69100	69100	69000
<b>Molar flow [kmol/hr]</b>	18500	1600	1600	1600	1600

*Table 12: CO<sub>2</sub> for sequestration*

The parameters of the CO<sub>2</sub>-rich stream going to storage are presented in table 12. It can be seen that the temperature in all cases is in the range of 91 to 188 °C. These temperatures are relatively moderate but still have to be taken into account when designing the storage facilities.

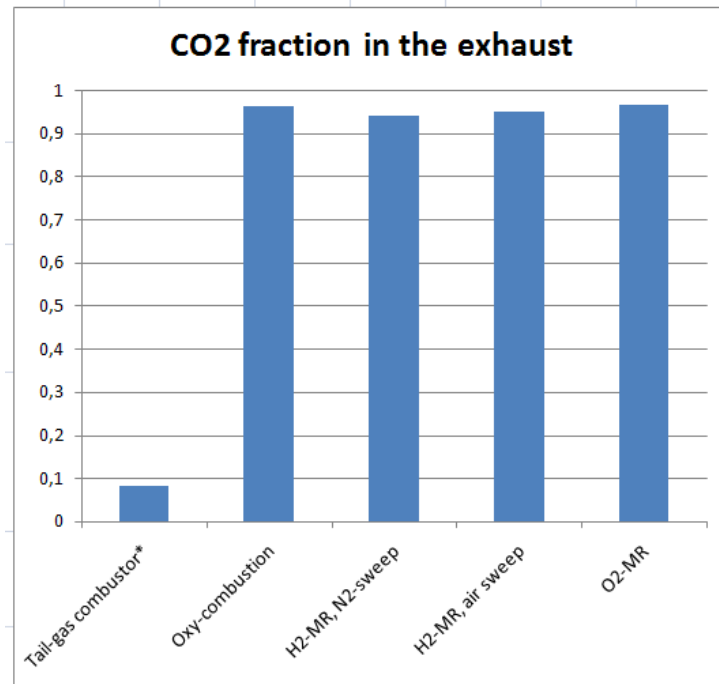


Figure 35: CO<sub>2</sub> fraction in the exhaust

If a simple mixing of anode and cathode streams is used to burn the fuel in the tail gas, the molar fraction of CO<sub>2</sub> would be below 10% (figure 35). If we use the other tail-gas concepts the molar fraction of CO<sub>2</sub> reaches 94-97%. Concentrations this high make it possible to directly capture and prepare this CO<sub>2</sub> for storage. Only water knock-out and compressing is required.

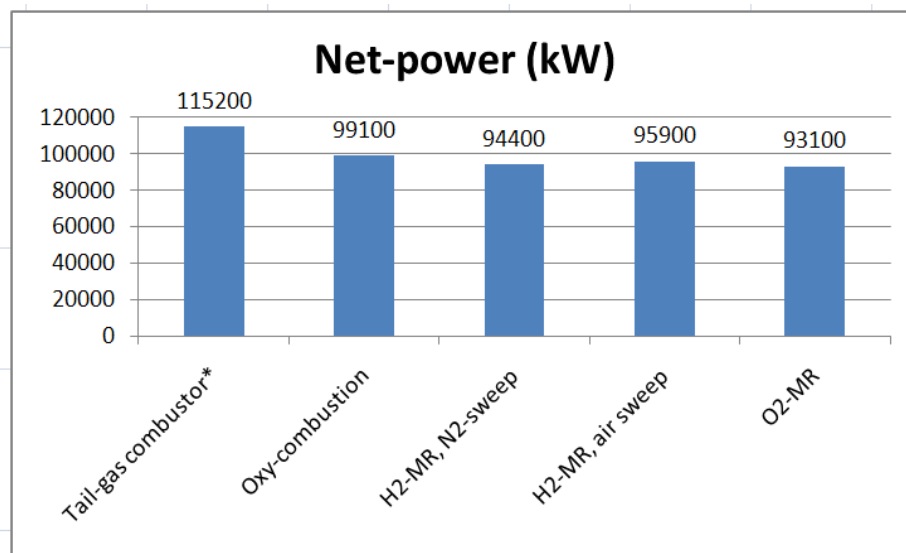


Figure 36: Net power production

The highest net power is achieved when the CO<sub>2</sub> is vented (figure 36). With CO<sub>2</sub> capture additional power is required for water knock-out and compression of CO<sub>2</sub> for storage. The DC power from the SOFC is 74,7 MW in all cases because the fuel parameters and utilization are the same. What varies is power output from the gas turbine, due to the different mass

flows and inlet temperatures of working fluid. The net power generated by the systems with CO<sub>2</sub> capture are almost equal, the difference is up to 6 MW.

The power generated by the systems with CO<sub>2</sub> capture is around 80% compared to when CO<sub>2</sub> is vented. But no CO<sub>2</sub> is captured.

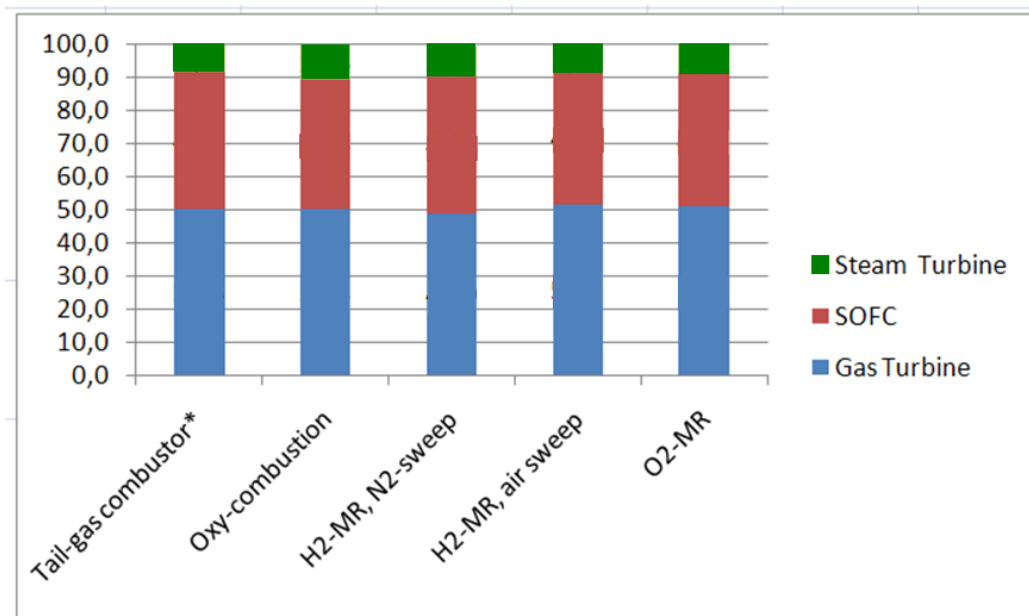


Figure 37: Power production breakdown

The power production breakdown of the created power system is presented in figure 37. As is visible, the bulk of the power is generated with the gas turbine and the SOFC. The Rankine steam cycle produces around 10 per cent of the total power. It should be considered whether it is reasonable to add the Rankine cycle to the system. That consideration is not possible for this thesis report because no cost estimates have been done.

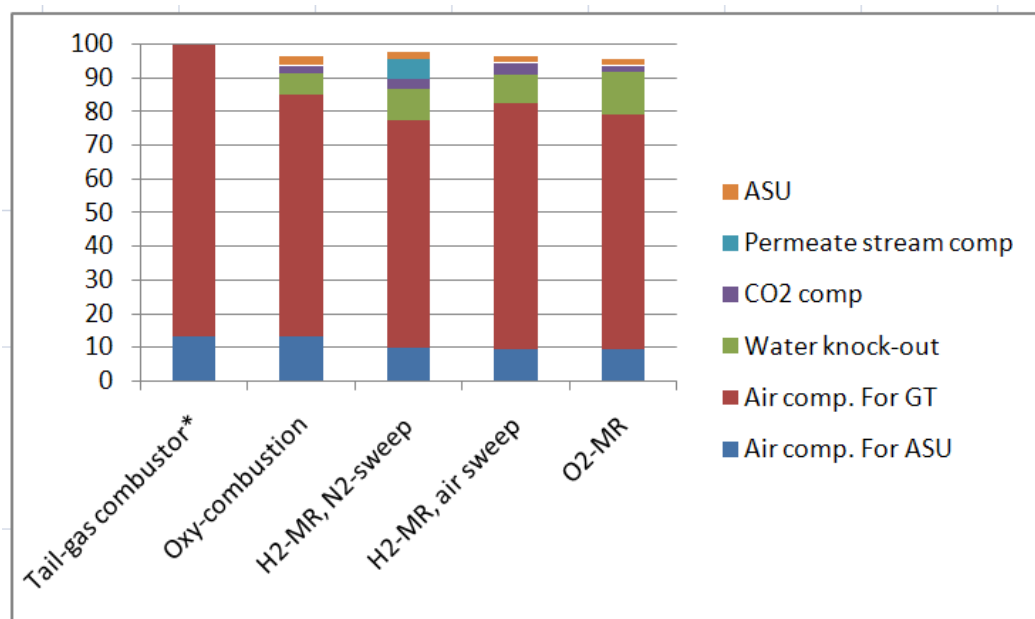
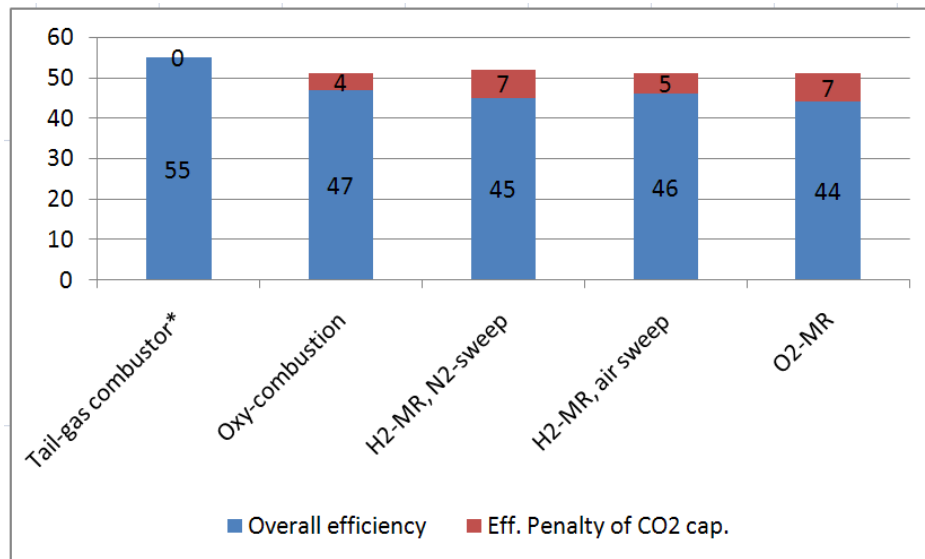


Figure 38: Power consumption breakdown

The breakdown of the power consumption (figure 38) shows that the majority of the overall power consumption of the plant comes from compressing the air. Some of it is used for the ASU but the main part is utilized for cooling the SOFC. The reason for compressing that much air is that that is how direct cooling with the air flow takes place. For future work the indirect cooling of the stack should be considered. This would decrease the amount of air needed to be compressed. The other places where power is needed play a significantly smaller part in the overall power consumption. It has to be kept in mind that changing the air flow to the stack may have affected the overall operation of the system e.g. flow of air is smaller and thus higher temperatures at the inlet of the gas turbine are achievable.

	<b>Tail-gas combustor*</b>	<b>Oxy-combustion</b>	<b>H<sub>2</sub>-MR, N<sub>2</sub>-sweep</b>	<b>H<sub>2</sub>-MR, air sweep</b>	<b>O<sub>2</sub>-MR</b>
<b>Overall efficiency (LHV)</b>	55	47	45	46	44

*Table 13: Overall efficiency [%]*



*Figure 39: Efficiency breakdown*

From the CO<sub>2</sub> capture concepts oxy-combustion shows the highest overall efficiency (table 13), but the others are not far behind, only up to 3 per cent points less. In the net power produced the difference is around 6 MW (figure 36). The highest efficiency is achieved when the CO<sub>2</sub> is vented; the efficiency is 8 per cent points higher compared to the concept using oxy-combustion.

The efficiencies of the different concepts are compared without taking into account the losses involved with water knock-out and compression of CO<sub>2</sub> (figure 39). Also, the highest efficiency belongs to the concept when CO<sub>2</sub> is vented. No water knock-out and compression of CO<sub>2</sub> takes place, but the difference between other concepts is only 3 per cent points compared to the most efficient one, which is the H<sub>2</sub>-conducting membrane with N<sub>2</sub> as sweep gas.



The highest penalty in efficiency, because of CO<sub>2</sub> capture, belongs to the systems which have an H<sub>2</sub>-conducting membrane with N<sub>2</sub> as sweep gas and the O<sub>2</sub>-conducting membrane, -7 per cent points (Figure 39).

As is seen in the results (figure 39), CO<sub>2</sub> capture has a penalty on the overall efficiency of the IGFC power plant. In addition, even if the power losses connected to CO<sub>2</sub> capture are not taken into account the overall efficiencies are lower compared to when CO<sub>2</sub> is vented. This is because if CO<sub>2</sub> is sent to storage, the mass flow through the gas turbine will be smaller (table 11), and even though the mass flow through the gas turbine of the CO<sub>2</sub> venting case is one of the smallest, it is compensated by the fact that less air has to be compressed and the net value of power produced/consumed by the gas turbine is bigger.

By comparing the penalties associated with CO<sub>2</sub> capture (table 13), the overall efficiency is some 8-11 per cent points lower. It is a significant difference, but this penalty may possibly be compensated with the implementation of a carbon tax because the reason for the drop in the efficiency comes mostly from the water knock-out and compression of CO<sub>2</sub>.

It has to be noted that in the Rankine cycle the heat source temperatures are in the range of 350-450°C. The efficiency of the Rankine cycles, which was chosen to be 30%, should be revised and set according to the temperatures of the heat sources.

From the different concepts available today the oxy-combustion for burning the tail-gas is the most promising one. This is because it is a mature and well-proven technology, and membranes are still being developed. On the other hand, if an O<sub>2</sub>-conducting membrane technology will prove itself it may take away the need for an ASU and thus decrease the investment costs of the plant. The membrane technology is promising and allows for simplification of the system, but as seen in figure 29 the flow sheet can get quite complex, if the temperature and operating pressure of the devices is different.

## APPENDIX A

### Brayton cycle [A.1]

The **Brayton cycle** is a thermodynamic cycle that describes the workings of the gas turbine engine, basis of the jet engine and others. It is named after George Brayton (1830–1892), the American engineer who developed it, although it was originally proposed and patented by Englishman John Barber in 1791. It is also sometimes known as the Joule cycle.

A Brayton-type engine consists of three components:

- A gas compressor
- A mixing chamber
- An expander

In the original 19th-century Brayton engine, ambient air is drawn into a piston compressor, where it is compressed; ideally an isentropic process. The compressed air then runs through a mixing chamber where fuel is added- a constant-pressure isobaric process. The heated (by compression), pressurized air and fuel mixture is then ignited in an expansion cylinder and energy is released, causing the heated air and combustion products to expand through a piston/cylinder- another ideally isentropic process. Some of the work extracted by the piston/cylinder is used to drive the compressor through a crankshaft arrangement.

The term Brayton cycle has more recently been given to the gas turbine engine. This also has three components:

- A gas compressor
- A burner (or combustion chamber)
- An expansion turbine

Ideal Brayton cycle:

- isentropic process - Ambient air is drawn into the compressor, where it is pressurized.
- isobaric process - The compressed air then runs through a combustion chamber, where fuel is burned, heating that air—a constant-pressure process, since the chamber is open to flow going in and out.
- isentropic process - The heated, pressurized air then gives up its energy, expanding through a turbine (or series of turbines). Some of the work extracted by the turbine is used to drive the compressor.
- isobaric process - Heat Rejection (in the atmosphere).

Actual Brayton cycle:

- adiabatic process - Compression.
- isobaric process - Heat Addition.

- adiabatic process - Expansion.
- isobaric process - Heat Rejection.

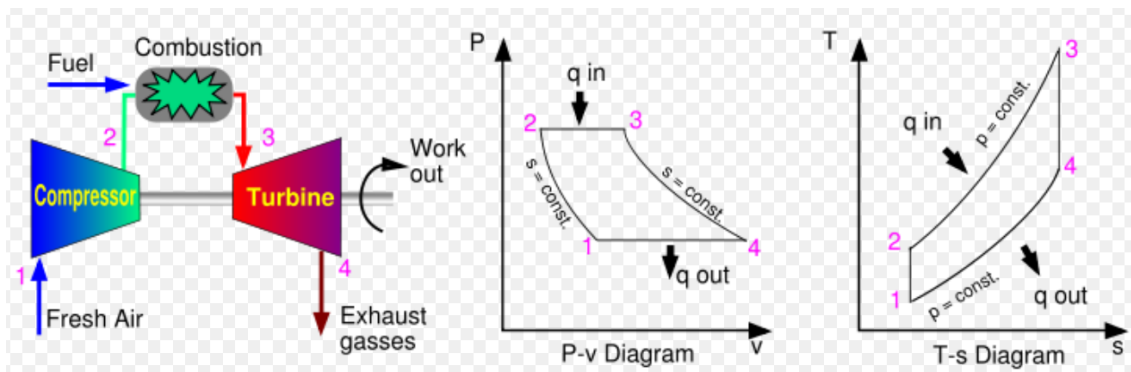
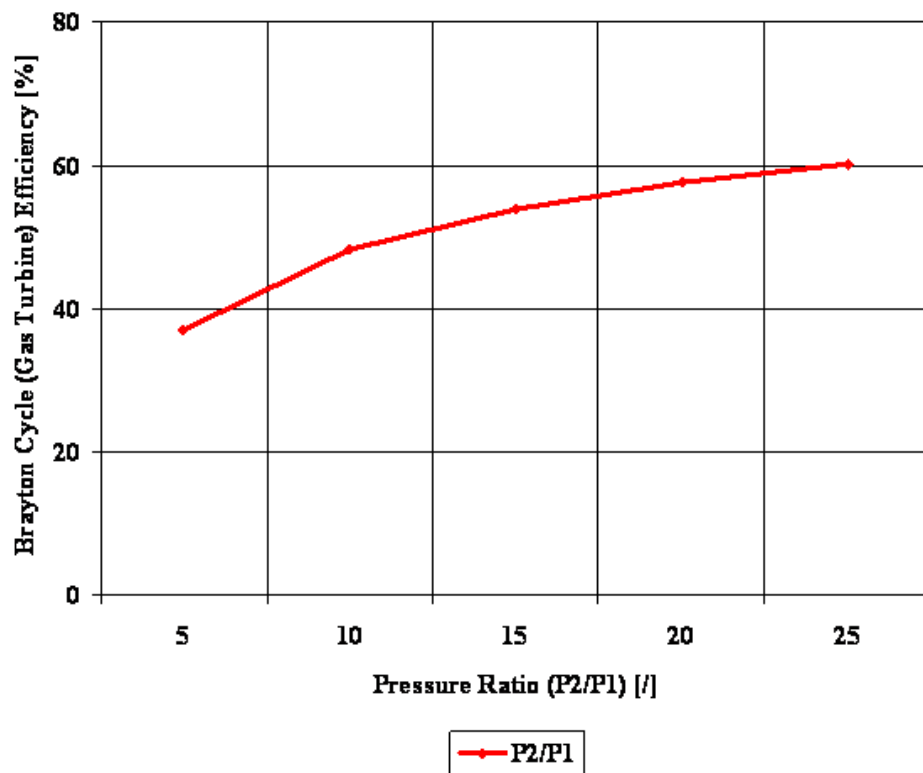


Figure 40: Idealized Brayton Cycle [1.15]

Since neither the compression nor the expansion can be truly isentropic, losses through the compressor and the expander represent sources of inescapable working inefficiencies. In general, increasing the compression ratio is the most direct way to increase the overall power output of a Brayton system.



Working Fluid: Air

Compressor Inlet Temperature: 298 [K] -- Gas Turbine Inlet Temperature: 1,500 [K]

Figure 41: Brayton Cycle (Gas Turbine) Efficiency

Here are two plots, Figure 42 and Figure 43, for the ideal Brayton cycle. One plot indicates how the cycle efficiency changes with an increase in pressure ratio, while the other indicates how the specific power output changes with an increase in the gas turbine inlet temperature for two different pressure ratio values.

In 2002 a hybrid open solar Brayton cycle was operated for the first time consistently and effectively with relevant papers published, in the frame of the EU SOLGATE program. The air was heated from 570 K to over 1000 K in the combustor chamber.

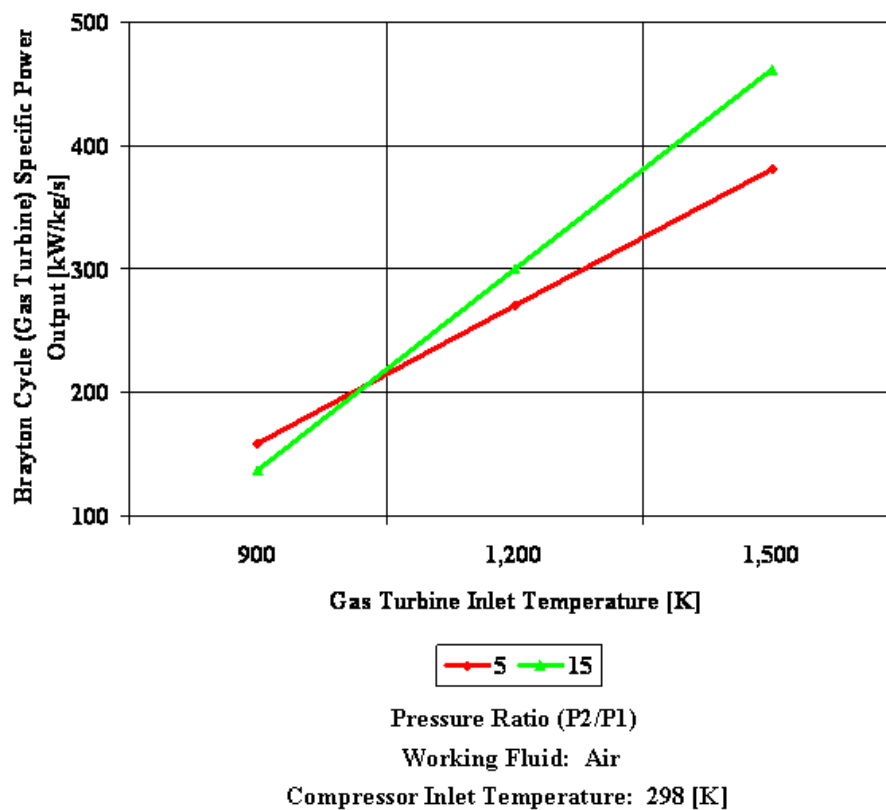


Figure 42: Brayton Cycle (Gas Turbine) Specific Power Output

## Methods to increase power

The power output of a Brayton engine can be improved in the following manners:

- **Reheat**, wherein the working fluid—in most cases air—expands through a series of turbines, then is passed through a second combustion chamber before expanding to ambient pressure through a final set of turbines. This has the advantage of increasing the power output possible for a given compression ratio without exceeding any metallurgical constraints (typically about 1000°C). The use of an afterburner for jet aircraft engines can also be referred to as *reheat*, it is a different process in that the reheated air is expanded through a thrust nozzle rather than a turbine. The metallurgical constraints are somewhat alleviated enabling much higher reheat temperatures (about 2000°C). The use of reheat is most often used to improve the specific power (per through put of air) and is usually associated with a reduction in efficiency. This is most pronounced with the use of after burners due to the extreme amounts of extra fuel used.

## Methods to improve efficiency

The efficiency of a Brayton engine can be improved in the following manners:

- **Intercooling**, wherein the working fluid passes through a first stage of compressors, then a cooler, then a second stage of compressors before entering the combustion chamber. While this requires an increase in the fuel consumption of the combustion chamber, this allows for a reduction in the specific volume of the fluid entering the second stage of compressors, with an attendant decrease in the amount of work needed for the compression stage overall. There is also an increase in the maximum feasible pressure ratio due to reduced compressor discharge temperature for a given amount of compression, improving overall efficiency.
- **Regeneration**, wherein the still-warm post-turbine fluid is passed through a heat exchanger to pre-heat the fluid just entering the combustion chamber. This directly offsets fuel consumption for the same operating conditions, improving efficiency. It also allows results in less power lost as waste heat.
- A Brayton engine also forms half of the **combined cycle** system, which combines with a Rankine engine to further increase overall efficiency.
- **Cogeneration** systems make use of the waste heat from Brayton engines, typically for hot water production or space heating.

## Reverse Brayton cycle

A Brayton cycle that is driven in reverse, via net work input, and when air is the working fluid, is the **air refrigeration cycle** or **Bell Coleman cycle**. Its purpose is to move heat rather than produce work. This air cooling technique is used widely in jet aircraft.

## Rankine cycle [A.2]

The Rankine cycle is a thermodynamic cycle which converts heat into work. The heat is supplied externally to a closed loop, which usually uses water as the working fluid. This cycle generates about 80% of all electric power used throughout the world, including all solar thermal, biomass, coal and nuclear power plants. It is named after William John Macquorn Rankine, a Scottish polymath. A Rankine cycle describes a model of the operation of steam heat engines most commonly found in power generation plants.

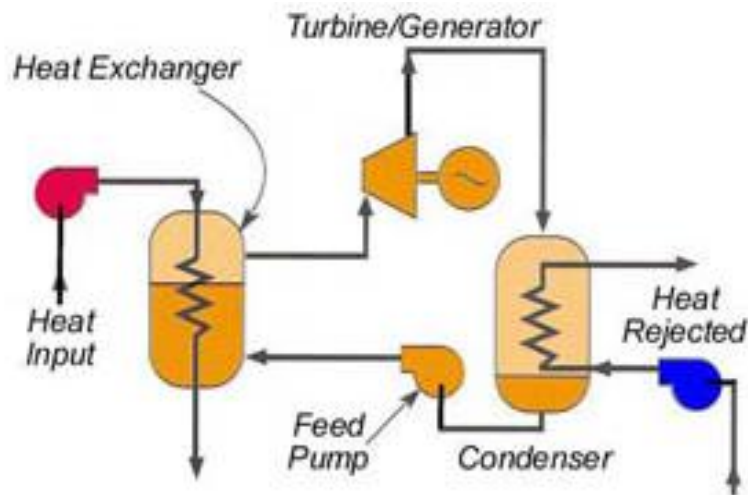


Figure 43: Engine with a Rankine cycle [1.18]

## Description

A Rankine cycle describes a model of the operation of steam heat engines most commonly found in power generation plants. Common heat sources for power plants using the Rankine cycle are coal, natural gas, oil, and nuclear.

The Rankine cycle is sometimes referred to as a practical Carnot cycle as, when an efficient turbine is used, the TS diagram will begin to resemble the Carnot cycle. The main difference is that a pump is used to pressurize liquid instead of gas. This requires about 100 times less energy than that compressing a gas in a compressor (as in the Carnot cycle).

The efficiency of a Rankine cycle is usually limited by the working fluid. Without the pressure going super critical, the temperature range the cycle can operate over is quite small. Turbine entry temperatures are typically 565°C (the creep limit of stainless steel) and condenser temperatures are around 30°C. This gives a theoretical Carnot efficiency of around 63% compared with an actual efficiency of 42% for a modern coal-fired power station. This low turbine entry temperature (compared with a gas turbine) is why the Rankine cycle is often used as a bottoming cycle in combined cycle gas turbine power stations.

The working fluid in a Rankine cycle follows a closed loop and is re-used constantly. The water vapor often seen billowing from power stations is generated by the cooling systems (not from the closed loop Rankine power cycle) and represents the waste heat that could not be converted to useful work. Note that steam is invisible until it comes in contact with cool, saturated air, at which point it condenses and forms the white billowy cloud seen leaving cooling towers. While many substances could be used in the Rankine cycle, water is usually the fluid of choice due to its favorable properties, such as nontoxic and unreactive chemistry, abundance, and low cost, as well as its thermodynamic properties.

One of the principal advantages it holds over other cycles is that during the compression stage relatively little work is required to drive the pump, due to the working fluid being in its liquid phase at this point. By condensing the fluid to liquid, the work required by the pump will only consume approximately 1% to 3% of the turbine power and give a much higher efficiency for a real cycle. The benefit of this is lost somewhat due to the lower heat addition

temperature. Gas turbines, for instance, have turbine entry temperatures approaching 1500°C. Nonetheless, the efficiencies of steam cycles and gas turbines are fairly well matched.

### Processes of the Rankine cycle

There are four processes in the Rankine cycle, each changing the state of the working fluid. These states are identified by number in the diagram to the right.

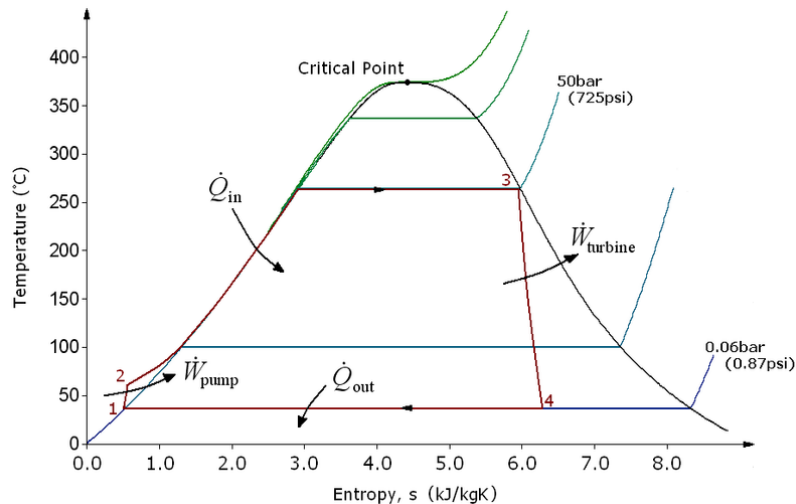


Figure 44: T-s diagram of a typical Rankine cycle operating between pressures of 0.06 bar and 50 bar

- **Process 1-2:** The working fluid is pumped from low to high pressure, as the fluid is a liquid at this stage the pump requires little input energy.
- **Process 2-3:** The high pressure liquid enters a boiler where it is heated at constant pressure by an external heat source to become a dry saturated vapour.
- **Process 3-4:** The dry saturated vapour expands through a turbine, generating power. This decreases the temperature and pressure of the vapour, and some condensation may occur.
- **Process 4-1:** The wet vapour then enters a condenser where it is condensed at a constant pressure and temperature to become a saturated liquid. The pressure and temperature of the condenser is fixed by the temperature of the cooling coils as the fluid is undergoing a phase-change.

In an ideal Rankine cycle the pump and turbine would be isentropic, i.e., the pump and turbine would generate no entropy and hence maximize the net work output. Processes 1-2 and 3-4 would be represented by vertical lines on the Ts diagram and more closely resemble that of the Carnot cycle. The Rankine cycle shown here prevents the vapor ending up in the superheat region after the expansion in the turbine, which reduces the energy removed by the condensers.

### Real Rankine cycle (non-ideal)

In a real Rankine cycle, the compression by the pump and the expansion in the turbine are not isentropic. In other words, these processes are non-reversible and entropy is increased during

the two processes. This somewhat increases the power required by the pump and decreases the power generated by the turbine.

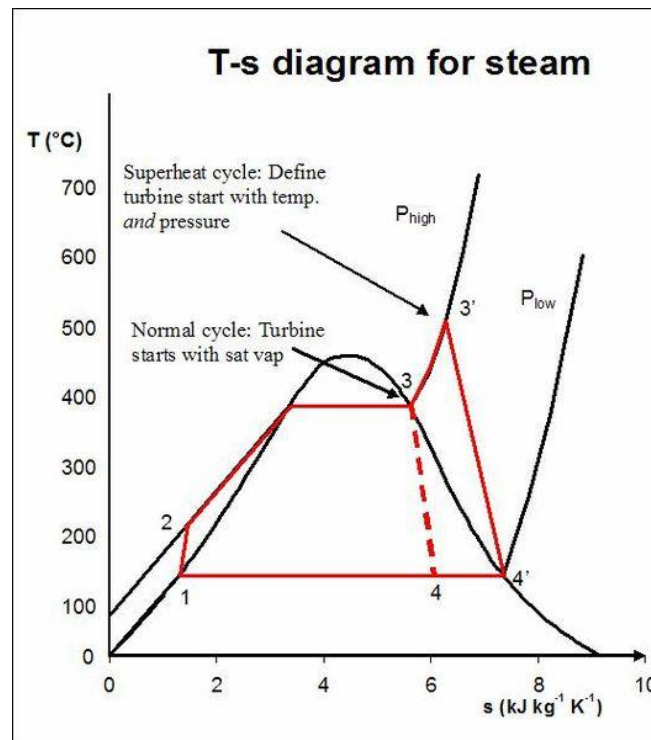


Figure 45: Rankine cycle with superheat

In particular the efficiency of the steam turbine will be limited by water droplet formation. As the water condenses, water droplets hit the turbine blades at high speed causing pitting and erosion, gradually decreasing the life of turbine blades and efficiency of the turbine. The easiest way to overcome this problem is by superheating the steam. On the Ts diagram above, state 3 is above a two phase region of steam and water so that, after expansion, the steam will be very wet. By superheating, state 3 will move to the right of the diagram and hence produce a dryer steam after expansion.

### Regenerative Rankine cycle

The regenerative Rankine cycle is so named because after emerging from the condenser (possibly as a subcooled liquid) the working fluid is heated by steam tapped from the hot portion of the cycle. On the diagram shown, the fluid at 2 is mixed with the fluid at 4 (both at the same pressure) to end up with the saturated liquid at 7. The Regenerative Rankine cycle (with minor variants) is commonly used in real power stations.



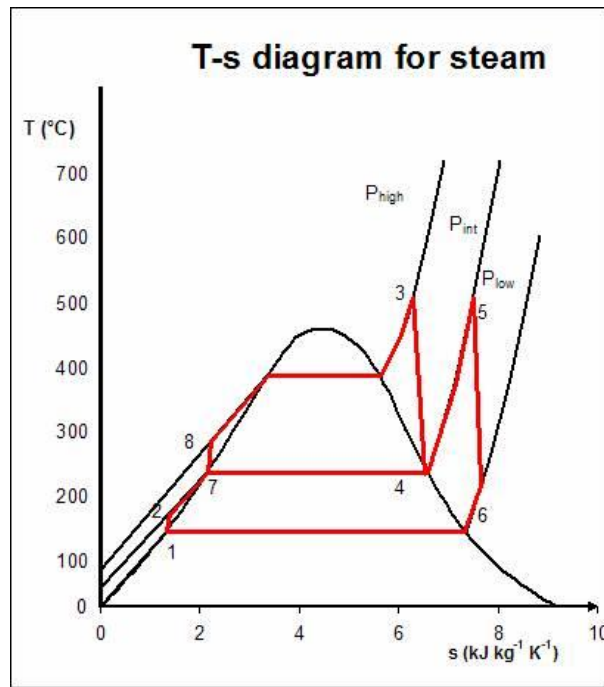


*Figure 46: Regenerative Rankine cycle*

Another variation is where 'bleed steam' from between turbine stages is sent to feed water heaters to preheat the water on its way from the condenser to the boiler.

### Appendix References

A.1 [http://en.wikipedia.org/wiki/Brayton\\_cycle](http://en.wikipedia.org/wiki/Brayton_cycle) - web page

A.2 [http://en.wikipedia.org/wiki/Rankine\\_cycle](http://en.wikipedia.org/wiki/Rankine_cycle) - web page

